Land-use related changes to sedimentary organic matter in tidal creeks of the northern Gulf of Mexico

Running head: Land-use change and sediment organic matter

Authors: Elizabeth S. Darrow[1,2,3], Ruth H. Carmichael[1,2], Kevin R. Calci[4], William Burkhardt III[4]

[1] Dauphin Island Sea Lab, 101 Bienville Blvd, Dauphin Island, AL 36528, USA

[2] University of South Alabama, Mobile, AL, 36688, USA

[3]Current Address: Elizabeth S. Darrow, Department of Biology & Marine Biology, University of North Carolina Wilmington, Center for Marine Science, 5600 Marvin K. Moss Lane, Wilmington, NC 28409, phone: (910) 962-7153, fax: (910) 962-4066, darrowe@uncw.edu

[4] US Food and Drug Administration, Gulf Coast Seafood Laboratory, 1 Iberville Drive, Dauphin Island, AL 36528, USA

Keywords: Stable isotope, nitrogen, carbon, *Clostridium perfringens*, indicators, ^{210}Pb, microtidal, tidal creek, sediment core

Type of Paper: Research Article

Abstract

Effects of land use on hydrology, organic matter sources and processing may be proportionately greater in tidal creeks than large estuaries, yet tidal creek systems have been undervalued in assessments of emerging effects of anthropogenic land use. Through sampling of dated sediment cores, we identified indicators of historical land use change (past 150 years) in a microtidal northern Gulf of Mexico tidal creek system in the early stages of urbanization. We found that tidal creeks differed from open water sites, and urbanized sites differed from less altered sites, primarily due to changes in carbon sources indicated by differences in sediment stable carbon isotope ($\delta^{13}C$) values, and concentrations of fecal indicator bacterium *Clostridium perfringens*. Total organic carbon (%TOC) and carbon:nitrogen (C:N) increased 2-fold in tidal creeks during upstream urbanization in the early 20th century, which led to elevated mid-century sediment TOC accumulation rates (5-10 mg C cm^{-2} y^{-1}), followed by decreases in TOC accumulation in tidal creeks and open waters since the 1960s (0.4-1.8 mg C cm^{-2} y^{-1}). *C. perfringens* and nitrogen stable isotope values ($\delta^{15}N$) were, respectively, 1.8 and 1.5 times higher at wastewater-influenced sites than at other sites, increasing through time or remaining high at wastewater-influenced sites from approximately the 1950s-present, when human populations quadrupled. Hence, urbanization altered estuarine inputs from upland C sources and increased inputs from human-derived N and microbes. These findings suggest that tidal creeks are more sensitive archives of land-use change than open water systems due to their proximity and greater connectivity to the watershed.

Introduction

Tidal creeks (riverine and semi-enclosed estuaries surrounded by salt marshes), found extensively through the Atlantic and Gulf coasts of North America (Chapman 1960), are important land-ocean transition zones. These waters provide ecosystem services such as habitat, buffer zones from storms and coastal erosion, and processing of land-derived nutrients (reviewed by Holland et al. 2004). Shellfish area closures from fecal contamination and loss of recreational and commercial fisheries value are also common in tidal creeks (Mallin and Lewitus 2004; DiDonato et al. 2009), which are in proximity to human activity and land use. Aside from a series of key studies in the southeast United States (*e.g.,* Sanger et al. 1999a, b; Holland et al. 2004), effects of urbanization on tidal creeks are not well understood, and areas of low population density or incipient urbanization have received even less attention.

Microtidal (<2 m tidal range, Davies and Moses 1964) estuaries and tidal creeks are worthy of study because they may function differently and be more sensitive to perturbation compared to larger, open systems. For example, estuarine phytoplankton biomass and response to nutrient loading (Monbet 1992), marsh sedimentation rates (Friedrichs and Perry 2001), and marsh carbon (C) flux (Chmura et al. 2011) appear to depend on tidal regime. Effects of land-use change on sediment supply, primary production, eutrophication, and marsh erosion seen in larger systems (Turner et al. 2006; Allison et al. 2007; Deegan et al. 2012) have not been adequately demonstrated in small subtropical estuaries. Furthermore, the varying inputs of nutrients, microbes, and organic matter to smaller systems (Anderson et al. 1997; Mulholland et al. 2008; Koop-Jakobsen and Giblin 2010) complicate predictions of water quality and ecosystem processes.

Hence, models for nitrogen (N) cycling, organic matter burial and diagenesis, and nutrient or C export to the coastal ocean developed for larger systems are unlikely to apply to smaller microtidal estuaries.

In addition, climate variation, severe storm events or sea level rise may have a greater affect on tidal creek systems. Severe storm events are common in subtropical climates and have potential to increase flooding, catastrophic infrastructure failures, stormwater inputs, and overflows of untreated wastewater (Rebich and Coupe, 2005, NPDES Permit AL0078921) in small ecosystems. Sea level rise increases the likelihood and severity of effects on microtidal estuaries by increasing rates of flooding and loss of landforms (Passeri et al. 2015; Kearney and Turner 2016). These events, in turn, can affect human health by increasing disease outbreaks and affecting safe fisheries harvest (Curriero et al. 2001). Smaller systems may also have climate-related functional differences in metabolic rates, flow regime, and other factors compared to temperate estuaries (*e.g.,* Caffrey 2004; Cloern et al. 2014), which affect susceptibility to perturbation. Determining sources of organic C, nutrients, and wastewater-derived microorganisms to tidal creek systems will add important terms to future nutrient budgets and public health assessments, and allow estimates of their importance under changing climate regimes on a global scale. Hence, it is important to expand studies to include smaller, tidal creek ecosystems that are in close proximity to human populations and among the estuarine environments most threatened globally (Kearney and Turner 2016).

Environmentally sound urbanization of the entire coastal zone is needed to support a functioning coupled human-ocean ecosystem (Halpern et al. 2012). While many ecosystems, particularly smaller microtidal systems, lack historical reference baseline

data, proxy data can be used to help define effects of urbanization on nutrient and organic matter sources and their fates (e.g. Davies and Bunting 2010; Smol 2010). Several sediment coring studies have been conducted to determine the effects of historical urbanization in large bays, harbors, and riverine systems adjacent to urban or residential centers (*e.g.,* Cornwell et al. 1996; Tucker et al. 1999; Bratton et al. 2003). Sedimentary biomarkers such as organic stable isotope ratios (δ^{15}N and δ^{13}C, *e.g.,* Zimmerman and Canuel 2002; Elliott and Brush 2006), C and N content, and spore-forming bacteria *Clostridium perfringens* (Abeyta et al. 1988; Skanavis and Yanko 2001) can identify historical nutrient sources (*e.g.*, wastewater, Tucker et al. 1999), effects on primary production (Peters et al. 1978; Fogel and Cifuentes 1993), and long-term C and N storage through organic matter burial (Bianchi and Allison 2009; Smith and Osterman 2014). For example, high δ^{15}N values can indicate N from processed wastewater, and lower δ^{13}C values are associated with terrestrial or freshwater C sources, compared to higher δ^{13}C values in marine or marsh-based systems. Although there may be hesitation to work in tidal creeks due to the possibility of physical disturbance in these shallow systems, proxies have been used with success (Table 1), and can provide information needed to evaluate changes in ecosystem and human health and guide suitable land-use (Halpern et al. 2012).

In this study, we measured spatiotemporal distributions of organic matter (C, N) and microbial source shifts related to land-use change in a subtropical microtidal estuarine system by measuring stable isotope ratios and fecal indicator bacteria in dated sediment cores, across tidal creeks and adjacent embayments of differing contemporary and historical land use. We estimated sediment organic C accumulation rates using ^{210}Pb-

derived sedimentation rates, which are not well documented for tidal creek systems. We hypothesized that in a microtidal estuarine system with varying human land uses, sediment C and N content and accumulation (organic matter inputs) would increase through time and be detectable as higher C accumulation rates in sediments in recent years (past 50 years) at sites more heavily impacted by land clearing, urbanization, and wastewater inputs. We anticipated sites with greater watershed urbanization through time to have lower $\delta^{13}C$ values due to increased routing of terrestrial organic matter downstream, while sites receiving processed wastewater inputs would have higher $\delta^{15}N$ values and *C. perfringens* concentrations in sediments. These results allow us to evaluate early fundamental effects of land-use change on C, N, and microbial inputs to tidal creeks of the northern Gulf of Mexico, and are useful to understand human influence on tidal creeks and small estuarine systems worldwide.

Materials and Methods

Study sites

Study sites were distributed across an hypothesized human impact gradient typical to the northern Gulf of Mexico, including four tidal creek sites within or near the Grand Bay National Estuarine Research Reserve (GBNERR): Bayou Heron (HE), Bayou Cumbest (CU), Bangs Lake (BA), Bayou Chico (CH). We compared these tidal creek systems to two nearby open water sites that served as endpoints, including 'unurbanized' Point aux Chenes Bay (PC) and 'urbanized' Bayou la Batre, Alabama (BB) (Fig. 1). While there is a gradient of land use and physical features, for comparison we grouped sites into general categories of "impacted" (outside GBNERR boundaries: CH, BB) or "reserve" (less impacted, within the GBNERR boundaries; BA, CU, HE, PC) based on watershed

population density and developed land cover; and as "creek" (CH, BA, CU, HE) or "open water" (PC, BB1, BB2) based on gross embayment attributes (Fig. 2). Developed land cover was specified using % impervious (hardened) surface within the watershed, which is an indicator for urbanization (Leopold 1968; Arnold and Gibbons 1996).

The GBNERR, located in southeastern Jackson County, Mississippi is characterized as a retrograding river delta estuary, with low freshwater flow and sediment load (Woodrey 2007a). Tidal creeks Bayou Heron, Bayou Cumbest and Bangs Lake are connected to Mississippi Sound, but are not part of a larger upstream river system (Kramer 1990; Otvos 2007). GBNERR is characterized by wet pine savanna uplands and *Juncus roemerianus* and *Spartina alterniflora* marsh. Although GBNERR has low population density and impervious surface, the reserve is fringed by encroaching residential development, industry, and septic and wastewater treatment plant (WTP) sewage sources, and is in the "intensifying" stage of land use transition (Foley et al. 2005; Darrow 2015). Population densities within GBNERR in 2010 were <0.1 persons ha^{-1}, equivalent to those in an early 1700's Chesapeake Bay watershed (Elliott and Brush 2006), but fringing areas had higher population densities up to 8.1 persons ha^{-1} (census data from Minnesota Population Center 2011).

Presently, the Bayou la Batre and Bayou Chico watersheds are serviced by municipal wastewater treatment plants (WTPs), and the Bayou la Batre WTP was the only permitted discharge for treated wastewater near our sites during the study period (NPDES Permit AL0078921, Fig. 1). The Bayou la Batre WTP processes human and seafood waste and releases effluent directly into Mississippi Sound. Bayou Chico in the neighboring city of Pascagoula also receives non-point wastewater inputs from residential and industrial

sources. Within the GBNERR, septic systems, boating areas, and localized industries are potential sources of human and industrial wastewater inputs, particularly to Bangs Lake, which is known to receive spill-water from a phosphate fertilizer processing facility (Blackburn 2000; Lytle and Lytle 2007). Point aux Chenes Bay, the unurbanized open-water reference site, is a shallow embayment within GBNERR, bordered by marsh and sand bars (Fig. 1).

Human land use in Grand Bay has been dated as early as 2500 years before present (Blitz and Mann 2000; Jackson 2012; Darrow 2015), but population growth in the Grand Bay region did not intensify until the late 19th century (Fig. 2). Although relatively little is known about the hydrology of the area, local and regional construction projects (*e.g.,* 1860s railroad, 1920s and 1960s highways) likely altered water flow from local creeks to the GBNERR (Woodrey 2007b; U.S. Army Corps of Engineers 2009). Infilling and hardening of the Point aux Chenes peninsula marshes occurred during industrial development in the 1950s (U.S. Geological Survey 1940, 1952, 1977). During 1955-1988, however, fringing industrial development increased, but agricultural land cover within GBNERR decreased and was replaced by increased forest and open water coverage. As a result, there was little net change in marsh land cover during this time (Shirley and Battaglia 2006).

Core sampling

To capture watershed and tidal sediment organic matter inputs, we collected cores from tidal creek sediments. Cores were collected during June 2011 in 1.0 – 1.5 m of water, using a vibracorer mounted on a pontoon barge (Stone and Morgan 1992) at all sites except at Bayou Chico, where cores were collected in June 2013 by hand from a

skiff due to narrower creek width. One core was analyzed from each site, except for Bayou la Batre, where two cores were collected 150 m (BB1) and 225 m (BB2) from shore to flank the wastewater discharge pipe. Cores of length > 1 m were collected with aluminum pipe (7.6 cm interior diameter). We took precautions to minimize sediment compaction during coring (thin-walled pipe, small diameter core-cutter, slow penetration rate, Morton and White 1997), but did not measure sediment compaction in the field. Cores were capped at top and bottom, and stored vertically while transported to the GBNERR lab. At the lab, water was siphoned from the top of the undisturbed core, the core was laid on its side, and the pipe was cut longitudinally. Sediment layers were measured and logged (color, texture, presence of shell or wood debris, Table S1). The entire core was sectioned in 2-cm increments. For each section sampled, 15.0 ± 0.2 g wet sediment was collected into sterile specimen cups on ice for *C. perfringens* analysis, and analyzed within 24 hours of collection. The remaining sediment was placed in pre-weighed, acid-washed and sterilized glass petri dishes. Wet weights were taken, and samples were stored frozen at -20°C until analysis. For analysis, the samples were dried at 60°C until constant weight (up to 1 week). Large pieces of debris were removed, then samples were homogenized by mortar and pestle and processed for sediment texture, radiometric dating, and stable isotope analysis.

Surface sediment and water column sampling

To determine relationships between water column and sediment organic matter stable isotope ratios, sediment and water samples were collected from each of nine sites, upstream and downstream of coring locations in June-September 2011 (Fig. 1). Water samples were collected using a Wildco horizontal seston sampler at 0.25 m above the

sediment surface, pre-filtered to remove particles >200 μm, transported on ice, then filtered at the lab onto pre-combusted glass fiber filters (0.7 μm nominal pore size). Surface sediment samples were collected using a sediment grab that was then sub-sampled with a modified syringe corer to collect three subsamples of the top 2 cm of sediment.

To evaluate physical connectivity between water column and the sediment, water column stratification was quantified by calculating static stability (E) using:

$$E = \frac{1}{\rho}\frac{\partial \sigma_{S,T,0}}{\partial z} \quad (1)$$

where $\sigma_{S,T}$ (density) (Gill 1982) used temperature and salinity measurements at depths (z) at the surface and 0.25 m from the bottom, measured with a YSI-85 while on station. Increasing stratification is represented by negative or positive deviations from zero.

Sediment texture analysis

Texture (grain size) was analyzed for each sediment sample by oxidizing organic material using 12% H_2O_2, wet-sieving (63 μm) to separate the sand fraction from fines, then using the pipette method (Folk 1974) to measure silt and clay fractions. Percentages of sand, silt, and clay were calculated as the proportion of total dry weight.

Radiometric dating

Dry sediment samples were analyzed by Microanalytica, LLC (Miami, FL) for particle-reactive radioisotopes ^{210}Pb and ^{137}Cs. Down-core activities of ^{210}Pb and ^{137}Cs were measured using direct γ -assay through an intrinsic germanium well detector (Ortec®), calibrated with a NIST traceable standard (IAEA-RGU-1). Supported ^{210}Pb is formed by in situ decay of ^{226}Ra, rather than deposition of ^{210}Pb from sinking particles. Supported ^{210}Pb was calculated by averaging activities of other ^{226}Ra daughter products

(^{214}Pb and ^{214}Bi) simultaneously with total ^{210}Pb within each layer (Joshi 1987). Selected samples from each core were measured for radioisotopes, reaching depths of supported levels of ^{210}Pb, and filling in extra analyses to achieve exponential decay profiles where possible.

Because there was potential for varying sedimentation rates through time, and for varying sediment texture to affect measured isotope activities, dates were calculated for sediment layers using three methods when possible, including ^{137}Cs first appearance, Constant Initial Concentration (CIC), and CIC normalized to sediment texture ($CIC_{normalized}$) (compared in Fig. S1). We used ^{137}Cs first appearance to evaluate ^{210}Pb-derived dates. Nuclear weapons testing beginning in 1954 released bomb-derived ^{137}Cs into the atmosphere, which settled into sediments. Hence, where ^{137}Cs was detectable, the deepest detectable ^{137}Cs was assigned a date of 1954 (Corbett et al. 2006; Smith and Osterman 2014). A constant accumulation rate was assumed to estimate dates between the 1954 ^{137}Cs appearance and the surface, using the ^{137}Cs half-life of 30.17 y.

For ^{210}Pb dates, we used the CIC model to determine date at a given sediment depth according to Appleby and Oldfield (1983), assuming that the ^{210}Pb flux and sediment accumulation rates were constant and any variability in ^{210}Pb concentrations, with the exception of decay, was averaged by sedimentological processes. We then modified the CIC model to normalize total ^{210}Pb for sediment texture by dividing total ^{210}Pb by percent fines (silt + clay) at each depth, as in Palinkas and Koch (2012) (details in Darrow 2015). Excess $^{210}Pb_{normalized}$ was calculated by subtracting supported $^{210}Pb_{normalized}$ from total $^{210}Pb_{normalized}$ (Fig. 3). CRS dates (allowing for changing sedimentation rates) were calculated for each depth using ^{210}Pb data according to Appleby and Oldfield (1983) and

Binford (1990). After comparing dates using all methods, we determined that texture-normalized ^{210}Pb dates and corresponding sedimentation rates using the $CIC_{normalized}$ model were the most reliable for this system.

Stable isotopes

To identify the modern sources of organic matter contributing to core sediments at each site, we measured C and N stable isotope ratios of WTP effluent and stormwater, suspended particulate matter from each site, and surface sediments.

Wastewater effluent was collected from three WTPs monthly near the study sites from May 2012 – May 2013. For stormwater, we conducted shoreline surveys for all actual and potential sources of pollution in May 2012, and Bayou Chico was the only tributary with drainage pipes/culverts visible above the water line. A subset of eight pollution sources in Bayou Chico was sampled for SPM during two time periods: May (dry weather) and June 2012 (within 24 h of a major storm event). WTP discharge and stormwater samples were sampled for stable isotopes using the same methods as for SPM from natural sources cited above.

Sediments and SPM on filters were dried in a 60ºC oven until a constant weight was achieved (sediment) or for 24 h (SPM). To remove inorganic carbon, sediment samples were acidified by fuming with 12.1 N HCl, re-dried, homogenized and 50–80 mg was packed into silver capsules before δ^{13}C analyses. Samples for δ^{15}N were packed in tin capsules, and analyzed separately from δ^{13}C samples because preliminary tests indicated that acid fumigation altered sediment δ^{15}N (standard deviation ± 1.02‰ among 26 duplicate pre-characterized samples). Samples were sent to the University of California Davis Stable Isotope Facility for analysis, where δ^{13}C and δ^{15}N and organic C and N

content were determined by continuous flow isotope ratio mass spectrometry (Elementar Vario EL cube elemental analyzer coupled to a Sercon 20-20 IRMS). $\delta^{13}C$ and $\delta^{15}N$ were measured relative to international standards (Vienna PeeDee Belemnite and atmospheric N_2, respectively). Reproducibility for 10 sediment samples analyzed in duplicate was 0.66 and 0.22 ‰ for $\delta^{13}C$ and $\delta^{15}N$, respectively. Reproducibility for five SPM samples analyzed in duplicate was 0.04 and 0.13 ‰ for $\delta^{13}C$ and $\delta^{15}N$, respectively.

Microbial indicator sampling

Wet sediment samples were analyzed for *C. perfringens* using a most-probable number quantification with iron-milk medium (Abeyta 1983; Abeyta et al. 1988). Briefly, 15 g sediment was diluted 1:10 with phosphate-buffered saline and vigorously stirred, pipetted into prepared iron-milk medium in a 5-tube multiple dilution series, and incubated in a 45.0ºC water bath for 18-24 hours. Positive tubes (indicated by "stormy fermentation") were counted and the most-probable number estimated using an MPN table (U.S Food and Drug Administration 2010).

Data analysis

To test whether *C. perfringens* inputs exceeded losses at the different sites and at different times, we measured deviations from an exponential decline down-core assuming a constant rate of diagenesis or senescence of *C. perfringens* down-core (constant net rate of decay = inputs – outputs). If surface inputs were constant through time, a non-conservative species would be expected to decay exponentially (Berner 1980). To compare decay rates in *C. perfringens* concentrations among sites, we performed linear regression on *ln*-transformed *C. perfringens* concentrations vs. sediment depth and tested for homogeneity of slopes. We then conducted analysis of covariance (ANCOVA)

followed by post-hoc Tukey's tests on sites with homogeneous slopes to test for differences in surface *C. perfringens* concentrations (intercept). To estimate correlations between core parameters among sites, we used a linear mixed model approach using the lmer function within the lme4 package (v.1.1-7, Bates et al. 2014 in R (R Core Development Team 2015). *P*-values were determined using type III ANOVA with the Satterthwaite approximation for denominator degrees of freedom in the lmerTest package v.2.0-2.5 in R. We used a linear mixed model with site as a random effect to estimate correlations between *C. perfringens* (fixed effect) and δ^{15}N levels. Similarly, we used lmer and lmerTest to estimate correlations between %TN and other parameters within cores, with site as a random effect. For correlations between water column and sediment isotope values across all sites, we used Pearson's *r*. Significance of results was determined using $\alpha = 0.05$ for all tests.

For principal components analysis, sediment core data were *ln*-transformed, and data were normalized to the mean for each parameter. Data were subjected to principal components analysis using the correlation matrix. Significant factors were selected based on eigenvalues >1 (Reid and Spencer 2009).

Results

Radiometric dating

The $CIC_{normalized}$ method estimated dates for PC, HE, CU, BB1, and CH for approximately 1920 – present day, based on mean ^{210}Pb-derived sedimentation rates adjusted for sediment texture, and verified using first appearance of ^{137}Cs (Fig. S1, Fig. 3, Table 2). Sediment texture (silt + clay content) was important to determining dates of sediment in cores because of variability in percent fines (generally increasing) down-core

(Table S1). Bulk densities increased down-core at all sites, except for tidal creek site CH, which did not have a major change in bulk density with depth (Table S1).

For most sites, sediment dates calculated using ^{137}Cs were within the error range of dates calculated using $CIC_{normalized}$ (based on ^{210}Pb), giving confidence to the $CIC_{normalized}$ method for these shallow systems with varying sediment type (Fig. S1). ^{137}Cs dates did not align with $CIC_{normalized}$ or CIC dates at BB2, even though the $CIC_{normalized}$ trendline was significant (Table 2, Fig. S1c, Fig. 3c). Cores from two sites (PC, CH) did not have measurable ^{137}Cs, so ^{137}Cs could not be used alone for dating at these sites. At the Bangs Lake (BA) site, ^{137}Cs was high to 18-20 cm (Table S1), and did not have a subsurface peak, but decreased exponentially from the surface. Excess ^{210}Pb had a subsurface peak near 10 cm at BA, indicating possible non-atmospheric sources of radionuclides that interfered with estimating dates for the BA core.

Sediment accumulation rates

Mean sediment accumulation rates based on $^{210}Pb_{normalized}$ ranged from 0.11 cm y^{-1} (BB2) to 0.86 cm y^{-1} (BA) (Table 2, Fig. 3). Open water sites (BB1, BB2, PC) had similar accumulation rates (mean 0.36 cm y^{-1}) to tidal creek sites (HE, CU, BA, CH, 0.43 mm y^{-1}). When tidal creek site BA was excluded based on possible radionuclide contamination (see Discussion), open water sites had a higher mean sediment accumulation rate than tidal creeks (HE, CU, CH, mean = 0.28 mm y^{-1}).

$^{210}Pb_{normalized}$ activity in sediments decreased exponentially with depth at all sites, reaching background ("supported") levels between 19 and 39 cm (Fig. 3). There was some evidence of physical mixing in the top of the Bayou Chico core (Fig. 3g), with excess $^{210}Pb_{normalized}$ activity varying to about 10 cm. Below 10 cm depth at CH,

$^{210}Pb_{normalized}$ decreased logarithmically, allowing extrapolation of dates for the top 10 cm of the core.

Down-core organic matter profiles

Percent total organic carbon content (%TOC) in sediments ranged from 0.076 (HE) to 2.60 (CH) %TOC (Fig. 4). %TOC was highest and showed greater variation down-core at tidal creek sites compared to open-water reference sites, but did not differ between reserve sites and more impacted sites off the reserve (Fig. 4, Table 3). All tidal creek sites had maximum %TOC mid-core, which was most pronounced at HE and CU between 20–40 cm depth (early 1900s). CH had high %TOC throughout, and open water sites PC, BB1, and BB2 had low and less variable %TOC than tidal creek sites.

%TN did not differ on average between tidal creek sites compared to open-water reference sites, or at impacted (CH, BB) compared to reserve sites because of high within-core variability (Table 3). Most tidal creek sites had high surface %TN, decreasing with depth (Fig. 4), and sediment %TN at urbanized tidal creek site CH was 2 times higher than other tidal creek sites. Open water site BB1 had maximum %TN between 20–40 cm (estimated 1950–1975), and BB2 (nearest the present-day WTP outfall) had higher %TN than the open-water sites PC and BB1.

Sediment C:N showed similar down-core trends to %TOC profiles (Fig. 4). C:N was higher at creek than open water sites, but was similar between impacted and reserve sites (Table 3). C:N maxima were observed at tidal creek sites at the same depths as high %TOC sections noted above, but open-water sites did not have prominent down-core C:N changes, other than a maximum C:N at the open-water site PC at the deepest depth (80 cm, ~1850, Fig. 4).

Down-core stable isotope ratios

$\delta^{13}C$ was the parameter explaining the most variability among core samples in the principal components analysis (Fig. 5, PC1 = 58.6% variability, loading for $\delta^{13}C$ = 0.98). Open water sites had higher $\delta^{13}C$ values on average than tidal creek sites (Table 3), and for example, reserve sites PC (open) and HE (creek) were differentiated primarily by $\delta^{13}C$ (Fig. 5). Open water sites BB1, BB2, and PC had down-core $\delta^{13}C$ profiles near -22 ± 1‰, indicating relative marine influence, while $\delta^{13}C$ in sediments from tidal creeks were lower (mean -24 to -25 ‰), consistent with terrestrial or needle rush (*Juncus roemerianus*) inputs (Fig. 4). There were periods of major shifts in $\delta^{13}C$ at tidal creek sites, but $\delta^{13}C$ did not help differentiate impacted vs. reserve sites (Figs. 4, 5; Table 3). At tidal creek sites CU, HE, and BA lower $\delta^{13}C$ (CU, HE: -27 to -29 ‰; BA: -25 ‰) was found in deeper layers, increasing towards the surface, with a change in values near 20–40 cm depth (~1950) concomitant with maxima in %TOC (Fig. 4). $\delta^{13}C$ in sediments from Sites BB1 and BB2 near the WTP outfall decreased by about 0.5 ‰ toward the surface (approx. 1960 to present). $\delta^{13}C$ in sediments at urbanized tidal creek CH was intermediate, ranging from -24 to -26 ‰ with no observable down-core pattern.

While there were no substantial differences in $\delta^{15}N$ between creek and open water sites, on average, $\delta^{15}N$ values in sediments at impacted sites were higher than at reserve sites, (Table 3). $\delta^{15}N$ was higher at wastewater outfall sites BB1 and BB2, and urbanized tidal creek site CH (average 4.07 - 5.10 ‰) compared to the open-water reserve site PC (2.34 ± 0.23‰). Tidal creek sites CU, BA, and HE had intermediate $\delta^{15}N$ values in sediments, ranging 2.85 to 3.47‰ (Fig. 4). $\delta^{15}N$ decreased with depth at human-impacted sites BB1, BB2 and CH, while reserve tidal creek sites showed no pattern down-core. At

tidal creek sites HE and BA, δ^{15}N became lower near 20 cm, then higher again towards the surface, with these shifts of 0.5 – 0.6 ‰ in the same depth layers as previously noted shifts in %TOC, %TN, and δ^{13}C.

Microbial indicator

While open-water and tidal creek sites were not different, *C. perfringens* explained a substantial amount of the variability among sites (loading for principal component 2 = 0.97, Fig. 5), with higher densities in sediments at impacted sites compared to reserve sites (Figs. 4, 5; Table 3b). In surface sediments, *C. perfringens* densities were high near known sewage impacted sites (BB1 and BB2, 9.2 x 10^3 MPN $100g^{-1}$), and densities were up to 10 times higher at urbanized Bayou Chico (1.3 x 10^4 MPN $100g^{-1}$, Fig. 4) than in sediments at less impacted tidal creek sites (HE: 2.4 x 10^3 MPN $100g^{-1}$). *C. perfringens* was ubiquitous (>10^4 MPN 100 g^{-1} sediment) throughout the 40 cm of the CH core. Among other sites, *C. perfringens* densities typically decreased exponentially with sediment depth (Fig. 4, linear regression of *ln*C. perfringens vs. depth; $p<0.03$ for all). Open-water reference site PC had the lowest surface concentrations of *C. perfringens* (4.9 x 10^2 MPN $100g^{-1}$), which decreased with depth to below detection limits at 14 cm and deeper (1990 and earlier). At HE and BB2, *C. perfringens* had higher concentrations deeper in the core than expected based on exponential decay alone. Cores from CH, CU, and BB1 showed non-steady-state behavior of *C. perfringens*, with periods of time that had major deviations from an exponential declining pattern down-core.

Surface sediment and suspended matter connectivity

Mean δ^{13}C and δ^{15}N values in surface sediments at upstream and downstream locations at each site were correlated with mean stable isotope values in bottom water

SPM (δ^{13}C: r = 0.75, p = 0.01; δ^{15}N: r = 0.82, p < 0.01, Fig. 6). Sediment δ^{13}C was higher by 2.99 ± 0.32‰ relative to SPM, with $\delta^{13}C_{SPM\text{-}Sed}$ ranging from -1.70‰ (Chico Upstream) to -4.64‰ (Cumbest Upstream) (Table 4). In contrast, sediment δ^{15}N was lower by 2.11 ± 0.11‰ relative to SPM, with $\delta^{15}N_{SPM\text{-}Sed}$ ranging from 0.22 (Heron Upstream) to 4.91‰ (Bangs). Of the physical factors analyzed (stratification, salinity, temperature, water depth, TOC and TN content), the difference between SPM and sediment δ^{15}N was most strongly negatively correlated with static stability (stratification) of the water column (r = -0.62, p = 0.08), while $\delta^{13}C_{SPM\text{-}Sed}$ was most strongly correlated with SPM TOC content (r = 0.60, p = 0.09), TN content (r = 0.60, p = 0.09), and C:N (r = 0.59, p = 0.1). Stratification was greatest at HEU and lowest at wind-dominated sites PC and BA (Table 4).

Organic source indicators

Treated wastewater from all three WTPs had similar mean δ^{13}C and C:N values, ranging from -23.07 to -23.77‰, and 6.08 – 6.33, respectively. Annual mean δ^{15}N in WTP effluent was facility-specific, varying from 3.57‰ (Pascagoula) to 8.27‰ (Bayou la Batre) (Table S2). Stormwater SPM flowing into Bayou Chico had lower δ^{13}C, higher C:N, and intermediate δ^{15}N compared to wastewater effluent (Table S2).

Sediment core N and C were correlated across sites, with highest values of both at urbanized tidal creek CH (Fig. 7). %TN had a significant fixed effect on %TOC (%TOC = 14.13* (%TN) – 0.01068; $F_{1,72}$ = 75.8, p <0.001, Fig. 7a), δ^{13}C (δ^{13}C = 14*(%TN) - 24.74; $F_{1,72}$ = 7.38, p <0.01, Fig. 7b), and *C. perfringens* (ln*C. perfringens* = 57.3*(%TN) + 2.36, $F_{1,72}$ = 21.4, p<0.001, Fig. 7c). The random effect of site was significant in each linear mixed model, demonstrating the importance of site-specific N and C sources. *C.*

perfringens and %TN values were low at reserve sites PC and HE, but both values were high at CH (Fig. 7c). Two potential wastewater indicators, *C. perfringens* and $\delta^{15}N$, were correlated across sites ($\delta^{15}N = 0.055* \ln C.\ perfringens + 3.245$; $F_{1,66} = 3.933$, $p = 0.05$; site included as random factor; Fig. 8).

For sediment samples that were successfully dated, C accumulation rates (sediment accumulation rate * bulk density * % TOC) varied among sites and through time (Fig. S2). Sediment layers prior to 1960 had significantly higher TOC accumulation rates than sediment layers post-1960 (ANOVA, $F_{1,35} = 9.2$, $p < 0.01$). Since approximately 1960, tidal creek TOC accumulation rates have declined to rates similar to open water sites, except for Bayou Chico, which had TOC accumulation rates up to three times higher than reserve tidal creek sites HE and CU (Fig. S2).

Discussion

There have been major changes in the sources and quantities of organic matter and N delivered to tidal creeks and open waters in and around the Grand Bay estuary system in the northern Gulf of Mexico during the past 100 years. These changes can be attributed to (1) historical alterations to the hydrology of tidal creek watersheds, and (2) increases in the number and magnitude of wastewater discharges into tidal creeks and open waters. We linked these processes to land-use change by relating the timing of compositional changes recorded in sediments to population increases and known historical events (Figs. 2 and 3, Table 5). Use of multiple indicators provided a powerful and explicit identifier of organic matter source shifts, and demonstrated that wastewater has become a dominant N and C source to urbanizing sites as land use changed in the Grand Bay region. The effects of land-use change on TOC and TN inputs were more detectable in the sediment

record at tidal creeks than at open water sites, despite historically higher sediment TOC and TN naturally occurring in tidal creek sites. Hence, tidal creeks were a sensitive recorder of information on anthropogenic-driven change in the Grand Bay estuary.

Hydrological alterations to watersheds

Patterns in sediment organic matter composition reflected changes in relative terrestrial influences and anthropogenic sources to the system. Major shifts in sediment %TOC, C:N, and organic C sources ($\delta^{13}C$) occurred during the same time period (1920s-1930s) in two tidal creeks (CU, HE, Table 5), indicating an ecosystem-level response to watershed alteration, because the two creeks were in separate sub-watersheds (W. Wu, unpubl.). Increased terrestrial organic matter inputs to sediments in the early 20th century were aligned in time with increased population growth (Fig. 2), construction of the railroad (1860s), Highway 90 (1920s), and Interstate-10 (1960s), which may have caused increased terrestrial runoff due to increased impervious surface. Accordingly, evidence for decreased terrestrial (upland) inputs (higher $\delta^{13}C$, decreasing C:N, %TOC and C accumulation rate) was detected in sediments during time periods after placement of railroad and highway berms, which reduced headwater flow from Franklin Creek (U.S. Army Corps of Engineers 2009).

These major modifications through the 20th century drastically reduced C burial by tidal creeks. Similar changes were observed later (mid-1960s, Table 5) at Bangs Lake (BA), when marshes were filled and converted to industrial areas (Eleuterius 1973), although the total marsh cover throughout GBNERR did not change during this time (Shirley and Battaglia 2006). A 40% reduction in agricultural land in the GBNERR watershed since the 1950s (Shirley and Battaglia 2006) and conversion to forest may also

help explain relative reductions in organic content of sediments seen in our data at CU and HE. Previous studies using sediment cores have also shown declines in delivery of terrestrial sediments downstream after highway and dam construction upstream (Allison et al. 2007; Smith et al. 2013) and marsh/tidal creek systems expanding and contracting due to land clearing and later cessation of agricultural activity (Kirwan et al. 2011). Although TOC burial declined, organic matter was retained and processed in situ rather than transported to open water areas, and tidal creeks better preserved the changing signatures of C and N sources associated with land-use change.

Wastewater sources of organic matter

Major changes in N source were attributable to human-derived wastewater at sites with higher population densities, but these changes were not seen at less altered reserve sites. Comparing organic source indicators to %TN allowed us to test for N-specific source relationships and determine whether indicator values were driven by similar processes among sites. Temporal and spatial increases in %TN, fecal indicator microbes, and δ^{15}N values in sediments (Table 5, Fig. 7) suggest wastewater as the dominant N source that increased historically relative to land-use intensity among sites. In response to major population growth in the 1950s-1960s (Fig. 2), Pascagoula and Bayou la Batre installed wastewater treatment infrastructure. Historical increases in wastewater inputs were most obvious at Bayou la Batre, where cores showed concurrent increases in δ^{15}N and *C. perfringens*, from the time direct sewage outfall began in 1972 (NPDES Permit AL0022632 1999-2004). Both BB sites had historically high δ^{13}C values, which then decreased towards the sediment surface as organic matter mixed with more WTP effluent through time (Table S2, Fig. 7b). High δ^{15}N values and *C. perfringens* densities in BB

sediments compared to all other sites corroborate the presence of a human-derived wastewater N source from the nearby WTP (Table S2, Fig. 7e).

Similarly, higher sediment δ^{15}N and *C. perfringens* were found in sediments from CH, which receives wastewater at unknown frequency due to failing infrastructure and consistent stormwater inputs. High concentrations of wastewater indicators were found as deep as 40 cm, representing the past 100 years, with periods of non-steady state behavior indicative of periods of higher *C. perfringens* inputs. For example, *C. perfringens* concentrations deep in HE and BB2 cores were higher than modeled inputs, likely reflecting periods of septic system failure (e.g., CU: 1996, LaSalle, 1997) or reduced WTP treatment efficiency. Hurricane Katrina completely inundated all WTPs in the area in 2005, and the Bayou la Batre WTP was not fully functional until a new facility was built in 2012 (NPDES permit reports 2005-2012). Elevated *C. perfringens* and δ^{15}N at BB correspond to these periods of failing infrastructure, highlighting the long-term influence of human wastewater to open-water and tidal creek areas fringing the Grand Bay system.

These changes are of concern because urbanization can disrupt connectivity between the landscape and marine ecosystem Grimm et al. (2008b). Specifically, urban stormwater could create short fast flow paths that decrease ecological coupling between terrestrial and aquatic components of the landscape. We found this type of response at urbanized Bayou Chico, where %TOC, %TN, and *C. perfringens* densities were high throughout the sediment record, and sediment profiles were much different than at the less impacted sites within the reserve. Greater inputs of N also likely increased autochthonous primary production at this site, as indicated by the increasing δ^{13}C of

sediment layers through time as has been seen in other systems (e.g., Meyers 1997; Turner et al. 2006; Macreadie et al. 2012). Other N sources and N-cycling processes likely contributed to variation in δ^{15}N at less impacted sites (particularly HE, CU, BA; light symbols, Figs. 7, 8). δ^{15}N values characteristic of atmospheric N fixation (e.g., Elliott and Brush 2006) and low *C. perfringens* densities in sediments at PC, for example, demonstrated that this bay has not undergone major N source shifts during the past ~100 years. In the absence of environmentally sensitive land use planning, however, tidal creeks and smaller estuary systems are susceptible to future alteration of land-sea relationships that can have significant effects on ecosystem and human health (Sanger et al. 1999b; Mallin et al. 2000; Holland et al. 2004).

Radionuclide indicators of industrial land-use change

The ^{210}Pb dating methods we used provided an unanticipated independent indicator of human influence on a tidal creek in this study. High sedimentation rates and down-core patterns of ^{137}Cs and ^{210}Pb observed at Bangs Lake were consistent with distribution of nuclides derived from the catchment, rather than solely atmospheric sources (Goodbred and Kuehl 1998). At BA, excess ^{210}Pb from the sediment surface could not be completely corrected by normalization to grain size, indicating radionuclide inputs from an outside source. The phosphate fertilizer plant in the Bangs Lake watershed has had controlled and uncontrolled releases of waste (Blackburn 2000), which can have high concentrations of uranium series radionuclides naturally present in raw phosphogypsum (Bolívar et al. 1995). Varying anthropogenic inputs of these nuclides would result in down-core increases in ^{210}Pb (San Miguel et al. 2003, 2004), like we observed. This approach, if more carefully calibrated, could help better determine sedimentation rates as well as

indicate contamination in tidal creeks or other coastal systems with phosphogypsum inputs.

Organic matter burial in tidal creeks

Grand Bay is a retrograding relict river delta with little sediment supply, and sediment accumulation rates were low and comparable to other microtidal, low energy estuaries in the northern Gulf of Mexico region (Table 1). Grand Bay sediment accumulation rates were similar to the Naples Bay estuary (Van Eaton et al. 2010), Charlotte Harbor, Florida (Turner et al. 2006), and Hillsborough Bay, a sediment-starved Tampa Bay sub-estuary (Brooks and Doyle 1998), but much lower than Tampa Bay proper (Santschi et al. 2001) and Apalachicola Bay (Surratt et al. 2008). Despite having similar sedimentation rates to open water sites (Fig. 3), tidal creek sites had 2-3 times higher TOC accumulation rates than open water sites (Table 1, Fig. S2), highlighting the importance of tidal creeks as estuarine C sinks. Land-use changes since the 1960s corresponded to lower TOC accumulation rates in most of the tidal creek sites. The exception was Bayou Chico (CH), which continued to have elevated sediment TOC accumulation due to a combination of high sediment accumulation rates and TOC content. This difference was probably due to greater urbanization and increased impervious surface in the Bayou Chico watershed, resulting in more rapid and direct delivery of sediment, organic matter, nutrients, and microbes. Land use has affected TOC accumulation rates differently at our study sites, depending on whether upstream sediment supply has weakened through time (CU, HE), or whether watershed alterations have increased sediment inputs to creeks (CH).

Climate-related shifts in organic matter

Along with land-use change, other factors may have contributed to organic matter changes in sediments through time and across sites, including sea level rise, storm events, and changing marsh inputs. At Grand Bay, the headlands and former barrier islands surrounding Point aux Chenes Bay (PC) eroded at a rate of 2.5–3 m y^{-1} in the 1990s (Schmid 2000), increasing open water by 5% from 1974–2001 (Hilbert 2006). At nearby Dauphin Island, AL, sea-level rise is estimated at 2.98 mm y^{-1} (Thatcher et al. 2013). Changes in $\delta^{13}C$ values in sediment at open water site PC were consistent with increases in marine relative to terrestrial organic matter inputs associated with sea-level rise. Increased influence of saltmarsh vegetation could also contribute to higher $\delta^{13}C$ values with sea level rise if area of marsh expanded; however, marsh expansion does not appear to have occurred in the Grand Bay system (Shirley and Battaglia 2006) and is unlikely under future sea level rise scenarios, which are expected to transport sediments seaward (Passeri et al. 2015). A similar pattern in $\delta^{13}C$ values was not seen at open-water sites BB1 and BB2 that were dominated by wastewater sources of N and C, suggesting wastewater-driven changes in sediment composition may mask effects of some natural drivers of change.

Hurricanes, common in the subtropical Gulf of Mexico, also could alter $\delta^{13}C$ values through either the sudden deposition of storm surge-derived sand and marine-derived (high $\delta^{13}C$) organic matter (Lambert et al., 2007) or transport of terrestrial debris from upland flooding (low $\delta^{13}C$). Bentley et al. (2002) found a 10 cm sand layer attributed to Hurricane Camille (1969) in Mississippi Sound cores ~ 40 km SW of GBNERR. We did not find evidence of hurricane-related deposition in ^{210}Pb data from any cores, but some tidal creek sites (HE, CU, CH) had sediment layers of higher percent sand and terrestrial

debris (Table S1, gray bars in Fig. 4). Stable isotope values, however, did not corroborate the source of deposited material, and the timing of these event layers was different for different creeks (earlier than 1916 for Bayou Heron and Bayou Cumbest; 1985 for Bayou Chico, Table S1). Hurricane occurrences were ruled as less likely than longer-term land-use change in affecting sediment composition during those periods.

Changes in sediment organic matter content and stable isotope values may occur due to changes in salt marsh cover and delivery rates of marsh-derived organic matter to local waters. It is currently unknown how relative distributions of the two major salt marsh macrophytes, *Juncus roemerianus* and *Spartina alterniflora*, have changed in Grand Bay through time. Because these plants have $\delta^{13}C$ values bracketing SPM values (*J. roemerianus:* -28‰, *S. alterniflora*: -14‰, Darrow 2015), varying mixtures of sediment organic matter from these plants could appear isotopically similar to phytoplankton (*e.g.,* marsh detritus near Bayou Heron: $\delta^{13}C$ = -20.58, Darrow 2015). In many systems, tidal creek suspended and sediment organic matter is mostly derived from plankton or terrigenous rather than marsh plant sources (Canuel et al. 1997; Boschker et al. 1999; Goñi et al. 2003). Given the prominence of *J. roemerianus* in the northern Gulf of Mexico, we suggest that future studies could use compound-specific stable isotope analysis to more discretely differentiate C sources to sediments in Grand Bay and similar microtidal systems. While upland development and associated impervious surface area in the watershed was the dominant land-use change in the Grand Bay system during the time periods analyzed for this study (Woodrey 2007b), changes in marsh area are likely to become increasingly important if urbanization or sea level rise alter hydrodynamics in

small estuaries to favor shorter flow paths (detected during this study) and offshore transport of sediments (Grimm et al. 2008; Passeri et al. 2015).

Relationships between water column and sediment organic matter

Assuming limited down-core diagenetic changes in stable isotope values, the sediment record is a reservoir of seasonally-, daily-, and tidally-varying SPM, anticipated to reflect a long-term average of isotope values in SPM after water-column processes (e.g., consumption, microbial respiration) have occurred. Our finding that surface sediments had lower δ^{15}N and higher δ^{13}C compared to SPM, is consistent with similar studies from a range of locations (Cifuentes et al. 1989; McClelland and Valiela 1998; Carmichael et al. 2004). These findings suggest that the SPM δ^{13}C signature changed with decomposition in the water column or the fine organic fraction was preferentially advected or resuspended by tidal currents. The decreased benthic-pelagic coupling of bottom water and sediments with increased static stability suggests a decoupling of particulate N flux from surface waters water to sediments when stratification occurs (Cifuentes et al. 1988). Differences in benthic-pelagic coupling are important to consider in microtidal creeks where tidal currents are relatively weak and may not mix the entire water column over a tidal cycle (Friedrichs and Perry 2001).

Conclusions

In subtropical tidal creeks of the northern Gulf of Mexico, watershed disruption of allochthonous organic carbon supply since the mid-20th century has been accompanied by evidence of increased nitrogen inputs and microbial contaminants from human wastewater sources. Proxy data from sediment cores allowed us to identify times when watershed impacts began, in a geographic area where there are few historical records of

water quality, hydrology, or ecological processes. In GBNERR, we found low sedimentation rates in marsh tidal creeks, but high sediment accumulation of organic C. While tidal creeks appear to be important TOC sinks in this subtropical, microtidal system, creeks may be losing their ability to provide sediment to the marsh surface due to decreased upstream sediment supply. TN inputs have increased at all GBNERR reserve sites, and increasing $\delta^{15}N$ associated with wastewater has increased since the mid-century watershed disturbances. Even at sites of relatively low human impact, the heritage of watershed disruptions due to land-use change was captured in tidal creek sediments. Tidal creeks in this subtropical microtidal system were more likely to retain signatures of altered wastewater and organic C sources than open water sites, rather than exporting them to coastal areas. Signatures of human impacts were also weaker in open water sites due to dilution in the water column and increased area for possible deposition. Hence, we have demonstrated that tidal creeks can function differently than open water sites in their responses to human influence such as wastewater inputs and watershed hydrological alterations. Similar to other studies, we found observable increases in $\delta^{15}N$ corresponding to historical and spatial increases in population density. Because effects of urbanization on $\delta^{15}N$ can be obscured by multiple N sources (WTP effluent, stormwater), *C. perfringens* was useful as a supplemental wastewater indicator. Wastewater inputs due to storm-related infrastructure failures and runoff are expected to continue in this subtropical system, with changes exacerbated in the future by watershed modifications and sea level rise.

Disruption of upstream flows by land-use change and increased impervious surface from urbanization will affect the ability of tidal creeks to act as landscape buffers and C

sinks through sediment accumulation. The shorter flow paths created through alteration of tidal creeks and increased occurrence of high precipitation events or sea level rise may deliver organic material more directly to coastal areas. Additional study on these sensitive transitional systems is needed to determine how the combination of landscape alteration and natural environmental variation will affect organic matter and nutrient fate in coastal ecosystems. Well-planned urbanization, including consideration for future capacity and maintenance of wastewater management infrastructure, is important to protect present day and near future water quality, reduce human health risks, support coastal economies, and maintain ecological function of coastal ecosystems.

References

Abeyta, C. J. 1983. Comparison of iron milk and official AOAC methods for enumeration of *Clostridium perfringens* from fresh seafoods. J. Assoc. Off. Anal. Chem. **66**: 1175–1177.

Abeyta, C. J., M. M. Wekell, C. A. Kaysner, R. F. Stott, E. V. Raghubeer, J. R. Matches, and J. T. Peeler. 1988. Media evaluation and behavior of *Clostridium perfringens* as an adjunct indicator of quality in shellfish growing areas. Water Sci. Technol. **20**: 63–70.

Alexander, R. B., R. a Smith, and G. E. Schwarz. 2000. Effect of stream channel size on the delivery of nitrogen to the Gulf of Mexico. Nature **403**: 758–762.

Allison, M. A., T. S. Bianchi, B. A. McKee, and T. P. Sampere. 2007. Carbon burial on river-dominated continental shelves: Impact of historical changes in sediment loading adjacent to the Mississippi River. Geophys. Res. Lett. **34**: L01606.

Anderson, I. C., C. R. Tobias, B. B. Neikirk, and R. L. Wetzel. 1997. Development of a process-based nitrogen mass balance model for a Virginia (USA) *Spartina alterniflora* salt marsh: implications for net DIN flux. Mar. Ecol. Prog. Ser. **159**: 13–27.

Appleby, P. G., and F. Oldfield. 1983. The assessment of ^{210}Pb data from sites with varying sediment accumulation rates. Hydrobiologia **103**: 29–35.

Arnold, C. L., and C. J. Gibbons. 1996. Impervious surface coverage: The emergence of a key environmental indicator. J. Am. Plan. Assoc. **62**: 243–258.

Bates, D., M. Mächler, B. Bolker, and S. Walker. 2014. Fitting Linear Mixed-Effects

Models using lme4. eprint arXiv:1406.5823

Bentley, S. J., T. R. Keen, C. A. Blain, and W. C. Vaughan. 2002. The origin and preservation of a major hurricane event bed in the northern Gulf of Mexico: Hurricane Camille, 1969. Mar. Geol. **186**: 423–446.

Berner, R. A. 1980. Early Diagenesis: A Theoretical Approach, Princeton University Press.

Bianchi, T. S., and M. A. Allison. 2009. Large-river delta-front estuaries as natural "recorders" of global environmental change. Proc. Natl. Acad. Sci. U. S. A. **106**: 8085–8092.

Binford, M. W. 1990. Calculation and uncertainty analysis of ^{210}Pb dates for PIRLA project lake sediment cores. J. Paleolimnol. **3**: 253–267.

Blackburn, B. R. 2000. The effects of industrial and cultural development on phytoplankton community dynamics within three bayou systems of Jackson County, Mississippi. University of Southern Mississippi.

Blitz, J. H., and C. B. Mann. 2000. Fisherfolk, Farmers and Frenchmen: Archaeological Investigations on the Gulf Coast, Mississippi Department of Archives and History.

Bolívar, J. P., R. García-Tenorio, and M. García-León. 1995. Enhancement of natural radioactivity in soils and salt-marshes surrounding a non-nuclear industrial complex. Sci. Total Environ. **173-174**: 125–136.

Boschker, H. T. S., J. F. C. de Brouwer, and T. E. Cappenberg. 1999. The contribution of macrophyte-derived organic matter to microbial biomass in salt-marsh sediments:

Stable carbon isotope analysis of microbial biomarkers. Limnol. Oceanogr. **44**: 309–319.

Bratton, J. F., S. M. Colman, and R. R. Seal. 2003. Eutrophication and carbon sources in Chesapeake Bay over the last 2700 yr: human impacts in context. Geochim. Cosmochim. Acta **67**: 3385–3402.

Brooks, G. R., and L. J. Doyle. 1998. Recent sedimentary development of Tampa Bay, Florida: A microtidal estuary incised into tertiary platform carbonates. Estuaries **21**: 391.

Caffrey, J. M. 2004. Factors controlling net ecosystem metabolism in U.S. estuaries. Estuaries **27**: 90–101.

Canuel, E. A., K. H. Freeman, and S. G. Wakeham. 1997. Isotopic compositions of lipid biomarker compounds in estuarine plants and surface sediments. Limnol. Oceanogr. **42**: 1570–1583.

Carmichael, R. H., B. Annett, and I. Valiela. 2004. Nitrogen loading to Pleasant Bay, Cape Cod: Application of models and stable isotopes to detect incipient nutrient enrichment of estuaries. Mar. Pollut. Bull. **48**: 137–143.

Chapman, V. J. 1960. Salt Marshes and Salt Deserts of the World, L. Hill.

Chmura, G. L., L. Kellman, and G. R. Guntenspergen. 2011. The greenhouse gas flux and potential global warming feedbacks of a northern macrotidal and microtidal salt marsh. Environ. Res. Lett. **6**: 044016.

Cifuentes, L. A., M. L. Fogel, J. R. Pennock, and J. H. Sharp. 1989. Biogeochemical

factors that influence the stable nitrogen isotope ratio of dissolved ammonium in the Delaware Estuary. Geochim. Cosmochim. Acta **53**: 2713–2721.

Cifuentes, L. A., J. H. Sharp, and M. L. Fogel. 1988. Stable carbon and nitrogen isotope biogeochemistry in the Delaware estuary. Limnol. Oceanogr. **33**: 1102–1115.

Cloern, J. E., S. Q. Foster, and A. E. Kleckner. 2014. Phytoplankton primary production in the world's estuarine-coastal ecosystems. Biogeosciences **11**: 2477–2501.

Corbett, D. R., B. McKee, and M. Allison. 2006. Nature of decadal-scale sediment accumulation on the western shelf of the Mississippi River delta. Cont. Shelf Res. **26**: 2125–2140.

Cornwell, J. C., D. J. Conley, M. Owens, and J. C. Stevenson. 1996. A sediment chronology of the eutrophication of Chesapeake Bay. Estuaries **19**: 488.

Curriero, F. C., J. A. Patz, J. B. Rose, and S. Lele. 2001. The association between extreme precipitation and waterborne disease outbreaks in the United States, 1948-1994. Am. J. Public Health **91**: 1194–1199.

Darrow, E. S. 2015. Biogeochemical and microbial indicators of land-use change in a Northern Gulf of Mexico Estuary. Doctoral Dissertation, University of South Alabama, Mobile, Alabama.

Davies, A. L., and M. J. Bunting. 2010. Applications of paleoecology in conservation. Open Ecol. J. **3**: 54–67.

Davies, J. L., and C. A. Moses. 1964. A morphogenetic approach to world shorelines. Zeitschrift für Geomorphol. **8**: 127–142.

Deegan, L. A., D. S. Johnson, R. S. Warren, B. J. Peterson, J. W. Fleeger, S. Fagherazzi, and W. M. Wollheim. 2012. Coastal eutrophication as a driver of salt marsh loss. Nature **490**: 388–92.

DiDonato, G. T., J. R. Stewart, D. M. Sanger, B. J. Robinson, B. C. Thompson, A. F. Holland, and R. F. Van Dolah. 2009. Effects of changing land use on the microbial water quality of tidal creeks. Mar. Pollut. Bull. **58**: 97–106.

Van Eaton, A. R., A. R. Zimmerman, J. M. Jaeger, M. Brenner, W. F. Kenney, and J. R. Schmid. 2010. A novel application of radionuclides for dating sediment cores from sandy, anthropogenically disturbed estuaries. Mar. Freshw. Res. **61**: 1268.

Eleuterius, L. N. 1973. The marshes of Mississippi, p. 149–190. *In* J.Y. Christmas [ed.], Cooperative Gulf of Mexico Estuarine Inventory and Study. Mississippi Gulf Coast Research Laboratory.

Elliott, E. M., and G. S. Brush. 2006. Sedimented organic nitrogen isotopes in freshwater wetlands record long-term changes in watershed nitrogen source and land use. Environ. Sci. Technol. **40**: 2910–2916.

Fogel, M. H., and L. A. Cifuentes. 1993. Isotope fractionation during primary production, p. 73–98. *In* M.S. Engel and S.A. Macko [eds.], Organic Geochemistry. Springer US.

Foley, J. A., R. Defries, G. P. Asner, C. Barford, G. Bonan, S. R. Carpenter, F. S. Chapin, M. T. Coe, G. C. Daily, H. K. Gibbs, J. H. Helkowski, T. Holloway, E. A. Howard, C. J. Kucharik, C. Monfreda, J. A. Patz, I. C. Prentice, N. Ramankutty, and P. K. Snyder. 2005. Global consequences of land use. Science **309**: 570–4.

Folk, R. L. 1974. Petrology of Sedimentary Rocks,.

Friedrichs, C. T., and J. E. Perry. 2001. Tidal salt marsh morphodynamics: A synthesis. J. Coast. Res. **SI**: 7–37.

Gill, A. E. 1982. Atmosphere-Ocean Dynamics, Academic Press.

Goñi, M. A., M. J. Teixeira, and D. W. Perkey. 2003. Sources and distribution of organic matter in a river-dominated estuary (Winyah Bay, SC, USA). Estuar. Coast. Shelf Sci. **57**: 1023–1048.

Goodbred, S. L., and S. A. Kuehl. 1998. Floodplain processes in the Bengal Basin and the storage of Ganges–Brahmaputra river sediment: an accretion study using ^{137}Cs and ^{210}Pb geochronology. Sediment. Geol. **121**: 239–258.

Grimm, N. B., D. Foster, P. Groffman, J. M. Grove, C. S. Hopkinson, K. J. Nadelhoffer, D. E. Pataki, and D. P. C. Peters. 2008. The changing landscape: ecosystem responses to urbanization and pollution across climatic and societal gradients. Front. Ecol. Environ. **6**: 264–272.

Gronberg, J. M., and N. E. Spahr. 2012. County-level estimates of nitrogen and phosphorus from commercial fertilizer for the conterminous United States, 1987-2006. U.S. Geological Survey Scientific Investigations Report 2012-5207.

Halpern, B. S., C. Longo, D. Hardy, K. L. McLeod, J. F. Samhouri, S. K. Katona, K. Kleisner, S. E. Lester, J. O'Leary, M. Ranelletti, A. A. Rosenberg, C. Scarborough, E. R. Selig, B. D. Best, D. R. Brumbaugh, F. S. Chapin, L. B. Crowder, K. L. Daly, S. C. Doney, C. Elfes, M. J. Fogarty, S. D. Gaines, K. I. Jacobsen, L. B. Karrer, H. M. Leslie, E. Neeley, D. Pauly, S. Polasky, B. Ris, K. St Martin, G. S. Stone, U. R.

Sumaila, and D. Zeller. 2012. An index to assess the health and benefits of the global ocean. Nature **488**: 615–20.

Hilbert, K. W. 2006. Land cover change within the Grand Bay National Estuarine Research Reserve: 1974–2001. J. Coast. Res. **226**: 1552–1557.

Holland, A. F., D. M. Sanger, C. P. Gawle, S. B. Lerberg, M. S. Santiago, G. H. . Riekerk, L. E. Zimmerman, and G. I. Scott. 2004. Linkages between tidal creek ecosystems and the landscape and demographic attributes of their watersheds. J. Exp. Mar. Bio. Ecol. **298**: 151–178.

Homer, C. G., J. A. Dewitz, L. Yang, S. Jin, P. Danielson, G. Xian, J. Coulston, N. D. Herold, J. D. Wickham, and K. Megown. 2015. Completion of the 2011 National Land Cover Database for the conterminous United States-Representing a decade of land cover change information. Photogramm. Eng. Remote Sens. **81**: 345–354.

Jackson, H. E. 2012. Archaeological investigations of coastal shell middens in the Grand Bay Estuary, Mississippi, Mississippi Department of Archives and History and the Mississippi Development Authority.

Joshi, S. 1987. Nondestructive determination of lead-210 and radium-226 in sediments by direct photon analysis. J. Radioanal. Nucl. Chem. **116**: 169–182.

Kearney, M. S., and R. E. Turner. 2016. Microtidal marshes: Can these widespread and fragile marshes survive increasing climate–sea level variability and human action? J. Coast. Res. **319**: 686–699.

Kirwan, M. L., A. B. Murray, J. P. Donnelly, and D. R. Corbett. 2011. Rapid wetland expansion during European settlement and its implication for marsh survival under

modern sediment delivery rates. Geology **39**: 507–510.

Koop-Jakobsen, K., and A. E. Giblin. 2010. The effect of increased nitrate loading on nitrate reduction via denitrification and DNRA in salt marsh sediments. Limnol. Oceanogr. **55**: 789–802.

Kramer, K. A. 1990. Late Pleistocene to Holocene geologic evolution of the Grand Batture headland area, Jackson County, Mississippi. Mississippi State University.

Lambert, W. J., P. Aharon, and A. B. Rodriguez. 2007. Catastrophic hurricane history revealed by organic geochemical proxies in coastal lake sediments: a case study of Lake Shelby, Alabama (USA). J. Paleolimnol. **39**: 117–131.

LaSalle, M. W. 1997. Water quality monitoring of shellfish growing waters and residential rock-reed wastewater treatment systems at Bayou Cumbest, Mississippi.

Leopold, L. B. 1968. Hydrology for urban land planning--A guidebook on the hydrologic effects of urban land use. Circular 1–18.

Lytle, T. F., and J. S. Lytle. 2007. Historical water quality, p. 72–77. *In* M.S. Peterson, G.L. Waggy, and M.S. Woodrey [eds.], Grand Bay National Estuarine Research Reserve: An Ecological Characterization2.

Macreadie, P. I., K. Allen, B. P. Kelaher, P. J. Ralph, and C. G. Skilbeck. 2012. Paleoreconstruction of estuarine sediments reveal human-induced weakening of coastal carbon sinks. Glob. Chang. Biol. **18**: 891–901.

Mallin, M. A., and A. J. Lewitus. 2004. The importance of tidal creek ecosystems. J. Exp. Mar. Bio. Ecol. **298**: 145–149.

Mallin, M. A., K. E. Williams, E. C. Esham, and R. P. Lowe. 2000. Effect of human development on bacteriological water quality in coastal watersheds. Ecol. Appl. **10**: 1047–1056.

McClelland, J. W., and I. Valiela. 1998. Linking nitrogen in estuarine producers to land-derived sources. Limnol. Oceanogr. **43**: 577–585.

Meyers, P. A. 1997. Organic geochemical proxies of paleoceanographic, paleolimnologic, and paleoclimatic processes. Org. Geochem. **27**: 213–250.

Minnesota Population Center. 2011. National Historical Geographic Information System: Version 2.0.

Monbet, Y. 1992. Control of phytoplankton biomass in estuaries: A comparative analysis of microtidal and macrotidal estuaries. Estuaries **15**: 563.

Morton, R. A., and W. A. White. 1997. Characteristics and corrections for core shortening in unconsolidated sediments. J. Coast. Res. **13**: 761–769.

Mulholland, P. J., A. M. Helton, G. C. Poole, R. O. Hall, S. K. Hamilton, B. J. Peterson, J. L. Tank, L. R. Ashkenas, L. W. Cooper, C. N. Dahm, W. K. Dodds, S. E. G. Findlay, S. V. Gregory, N. B. Grimm, S. L. Johnson, W. H. McDowell, J. L. Meyer, H. M. Valett, J. R. Webster, C. P. Arango, J. J. Beaulieu, M. J. Bernot, A. J. Burgin, C. L. Crenshaw, L. T. Johnson, B. R. Niederlehner, J. M. O'Brien, J. D. Potter, R. W. Sheibley, D. J. Sobota, and S. M. Thomas. 2008. Stream denitrification across biomes and its response to anthropogenic nitrate loading. Nature **452**: 202–205.

Otvos, E. G. 2007. Geological framework and evolutionary history, *In* M.S. Peterson, G.L. Waggy, and M.S. Woodrey [eds.], Grand Bay National Estuarine Research

Reserve: An Ecological Characterization. Grand Bay National Estuarine Research Reserve.

Palinkas, C. M., and E. W. Koch. 2012. Sediment accumulation rates and submersed aquatic vegetation (SAV) distributions in the mesohaline Chesapeake Bay, USA. Estuaries and Coasts **35**: 1416–1431.

Passeri, D. L., S. C. Hagen, M. V. Bilskie, and S. C. Medeiros. 2015. On the significance of incorporating shoreline changes for evaluating coastal hydrodynamics under sea level rise scenarios. Nat. Hazards **75**: 1599–1617.

Peters, K. E., R. E. Sweeney, and I. R. Kaplan. 1978. Correlation of carbon and nitrogen stable isotope ratios in sedimentary organic matter. Limnol. Oceanogr. **23**: 598–604.

R Core Development Team. 2015. R: A language and environment for statistical computing.

Rebich, R. A., and R. H. Coupe. 2005. Bacteriological and water-quality data collected at coastal Mississippi sites following Hurricane Katrina, September-October 2005.

Reid, M. K., and K. L. Spencer. 2009. Use of principal components analysis (PCA) on estuarine sediment datasets: The effect of data pre-treatment. Environ. Pollut. **157**: 2275–2281.

San Miguel, E. G., J. P. Bolivar, and R. Garcia-Tenorio. 2004. Vertical distribution of Th-isotope ratios, ^{210}Pb, ^{226}Ra and ^{137}Cs in sediment cores from an estuary affected by anthropogenic releases. Sci. Total Environ. **318**: 143–157.

San Miguel, E. G., J. P. Pérez-Moreno, J. P. Bolívar, and R. García-Tenorio. 2003.

Validation of isotope signatures in sediments affected by anthropogenic inputs from uranium series radionuclides. Environ. Pollut. **123**: 125–130.

Sanger, D. M., A. F. Holland, and G. I. Scott. 1999a. Tidal creek and salt marsh sediments in South Carolina coastal estuaries: II. Distribution of organic contaminants. Arch. Environ. Contam. Toxicol. **37**: 458–471.

Sanger, D. M., A. F. Holland, and G. I. Scott. 1999b. Tidal creek and salt marsh sediments in South Carolina coastal estuaries: I. Distribution of trace metals. Arch. Environ. Contam. Toxicol. **37**: 445–457.

Santschi, P. H., B. J. Presley, T. L. Wade, B. Garcia-Romero, and M. Baskaran. 2001. Historical contamination of PAHs, PCBs, DDTs, and heavy metals in Mississippi River Delta, Galveston Bay and Tampa Bay sediment cores. Mar. Environ. Res. **52**: 51–79.

Schmid, K. 2000. Shoreline erosion analysis of Grand Bay marsh.

Shirley, L. J., and L. L. Battaglia. 2006. Assessing vegetation change in coastal landscapes of the northern Gulf of Mexico. Wetlands **26**: 1057–1070.

Skanavis, C., and W. A. Yanko. 2001. *Clostridium perfringens* as a potential indicator for the presence of sewage solids in marine sediments. Mar. Pollut. Bull. **42**: 31–35.

Smith, C. G., and L. E. Osterman. 2014. An evaluation of temporal changes in sediment accumulation and impacts on carbon burial in Mobile Bay, Alabama, USA. Estuaries and Coasts **37**: 1092–1106.

Smith, C. G., L. E. Osterman, and R. Z. Poore. 2013. An examination of historical

inorganic sedimentation and organic matter accumulation in several marsh types within the Mobile Bay and Mobile—Tensaw River Delta region. J. Coast. Res. **63**: 68–83.

Smol, J. P. 2010. The power of the past: using sediments to track the effects of multiple stressors on lake ecosystems. Freshw. Biol. **55**: 43–59.

Stone, G. W., and J. P. Morgan. 1992. Jack-up pontoon barge for vibracoring in shallow water. J. Sediment. Res. **62**: 739–741.

Surratt, D., J. Cherrier, L. Robinson, and J. Cable. 2008. Chronology of sediment nutrient geochemistry in Apalachicola Bay, Florida (U.S.A.). J. Coast. Res. **243**: 660–671.

Thatcher, C. A., J. C. Brock, and E. A. Pendleton. 2013. Economic vulnerability to sea-level rise along the northern U.S. Gulf Coast. J. Coast. Res. **63**: 234–243.

Tucker, J., N. Sheats, A. E. Giblin, C. S. Hopkinson, and J. P. Montoya. 1999. Using stable isotopes to trace sewage-derived material through Boston Harbor and Massachusetts Bay. Mar. Environ. Res. **48**: 353–375.

Turner, R. E., N. N. Rabalais, B. Fry, N. Atilla, C. S. Milan, J. M. Lee, C. Normandeau, T. A. Oswald, E. M. Swenson, and D. A. Tomasko. 2006. Paleo-indicators and water quality change in the Charlotte Harbor Estuary (Florida). Limnol. Oceanogr. **51**: 518–533.

U.S Food and Drug Administration. 2010. Most probable number from serial dilution. Bacteriol. Anal. Man. Appendix 2.

U.S. Army Corps of Engineers Mobile District. 2009. Mississippi Coastal Improvements

Program (MsCIP): Hancock, Harrison, and Jackson Counties, Mississippi. Comprehensive plan and integrated programmatic environmental impact statement.

U.S. Geological Survey. 1940. Project Q00000, Image ID 90518.

U.S. Geological Survey. 1952. Project TE0000, Image ID 120006.

U.S. Geological Survey. 1977. Project VDVJIO, Image ID 580636.

Woodrey, M. S. 2007a. Introduction, *In* M.S. Peterson, G.L. Waggy, and M.S. Woodrey [eds.], Grand Bay National Estuarine Research Reserve: An Ecological Characterization. Grand Bay National Estuarine Research Reserve.

Woodrey, M. S. 2007b. Hydrology, *In* M.S. Peterson, G.L. Waggy, and M.S. Woodrey [eds.], Grand Bay National Estuarine Research Reserve: An Ecological Characterization. Grand Bay National Estuarine Research Reserve.

Zimmerman, A. R., and E. A. Canuel. 2000. A geochemical record of eutrophication and anoxia in Chesapeake Bay sediments: anthropogenic influence on organic matter composition. Mar. Chem. **69**: 117–137.

Acknowledgments

Work was funded by the NOAA NERR Science Collaborative (NOAA NA09NOS4190153) and the Dauphin Island Sea Lab/ US Food and Drug Administration Graduate Fellowship Program. We would like to thank the following for field and lab assistance: A Aven, IEB Condon, DJ Dalrymple, J Delo, G Doup, A Ellenburg, E Hieb, J Ivory, A Knobloch, J McFadyen, H Patterson, C Seeley, N Taylor. Thank you to J Cebrian, J Lehrter, R Kiene, S Kuehl, and C Mohrherr for advice and technical expertise. Comments by three anonymous reviewers increased the quality of this manuscript. The authors declare no conflict of interest.

Figure Legends

Figure 1. Site map of sediment coring locations (triangles) in the Grand Bay National Estuarine Research Reserve, MS (GBNERR, hatched), and surrounding areas. From west to east: Bayou Chico (CH), Bangs Lake (BA), Bayou Cumbest (CU), Point aux Chenes Bay (PC), Bayou Heron (HE), Bayou la Batre (BB1 and BB2). Circles and italicized site names are sites where suspended particulate matter (SPM) samples were collected, with "U" designating an upstream site in each tributary. Squares are locations of present-day wastewater treatment plants Pascagoula (PAS), Moss Point (MP), and Bayou la Batre (BLB). Heavy black diagonal lines represent highways and railroads.

Figure 2. (A) Population density of Jackson County, MS through the time (2010 census data: Minnesota Population Center 2011). Major population increases were in early 1900s, 1950s, and 1990s. (B) Coring sites characterized by 2011 population density vs. impervious surface for each watershed (impervious surface land cover data: Homer et al. 2015). These data, plus GBNERR boundaries, led to site designations of "reserve" (PC, HE, CU, BA) or "impacted" (CH, BB). (C) Jackson County fertilizer use, 1987-2006 (Gronberg and Spahr 2012).

Figure 3. Total and excess ^{210}Pb activity (disintegrations per minute per gram dry sediment, dpm g^{-1}), normalized for sediment texture (silt + clay content, see methods) vs. depth down-core at each site. Excess $^{210}Pb_{normalized}$ (Total – Supported $^{210}Pb_{normalized}$) was used to calculate sediment accumulation rates and dates using an exponential regression (Table 2). Mean sediment accumulation rate is inset on lower right for each site. *Calculated accumulation rate for BA may be inaccurate due to contamination by phosphogypsum –processing facility, artificially elevating ^{210}Pb (see Discussion for details).

Figure 4. Down-core profiles of sediment %TOC, %TN, $\delta^{13}C$, $\delta^{15}N$, *C. perfringens* and molar C:N with sediment depth. Estimated date ($CIC_{normalized}$ method) on right-hand y-axis. Open-water sites (top to bottom: PC, BB1, BB2), followed by tidal creek sites (HE, CU, BA, CH). Gray shaded bars where changes in sediment grain size, %TOC and C:N were noted, possibly hurricane event layers. For *C. perfringens*, lower and upper detection limits indicated by vertical dashed lines; samples below detection limits: white symbols. Significant regressions have lines of best fit as solid lines; dashed lines of best fit are used to demonstrate non-steady state periods.

Figure 5. Principal components analysis: *C. perfringens*, %TOC, %TN, $\delta^{13}C$, $\delta^{15}N$, % sand, % water. Symbols represent sediment core samples from different sites. Component 1 explained 58.6% of the variance (eigenvalue = 3.29); Component 2 explained 38.1% of the variance (eigenvalue = 2.14). Component 1 was primarily explained by $\delta^{13}C$ (loading = 0.98), and Component 2 was primarily explained by *C. perfringens* (loading = 0.97). $\delta^{13}C$ separated open water (PC, BB1, BB2) from tidal creek sites (CH, CU, HE), with BA intermediate. *C. perfringens* separated reserve (PC, HE, BA) from impacted sites (CH, BB1, BB2) with site CU intermediate.

Figure 6. Mean values for (a) $\delta^{13}C$ and (b) $\delta^{15}N$ of organic matter from surface sediments (y-axes) plotted against values from suspended particulate matter (SPM; x-axes) for locations downstream or upstream (indicated by UP in the legend) from each of the coring sites. Each point is an average of 3 replicate samples for sediment and SPM. Samples were collected in May-September 2011. SPM had consistently lower $\delta^{13}C$ and higher $\delta^{15}N$ than sediments, as indicated by 1:1 lines (dashed). Upstream sites had lower $\delta^{13}C$ than downstream sites, but upstream-downstream patterns were not evident for $\delta^{15}N$.

Figure 7. Comparisons between sediment core characteristics and %TN. Sites are grouped by hypothesized anthropogenic impact: more (dark symbols) to less (white symbols). C:N and stable isotope values are indicated for three potential anthropogenic organic matter sources (Bayou Chico stormwater, Bayou la Batre WTP effluent, Pascagoula WTP effluent).

Figure 8. Correlation between potential wastewater indicators δ^{15}N and ln(*C. perfringens*) densities for all sites and sediment core layers. Symbols for hypothesized wastewater-influenced sites are black; hypothesized non-wastewater-influenced sites have white symbols; We hypothesize that Bayou Cumbest is impacted by intermediate wastewater influence (gray symbols

Table 1. Literature sedimentation rate comparison for Gulf of Mexico microtidal estuarine sites.

Estuary	Site name	Estuary type	Sediment type	Sediment accumulation rate (cm year^{-1})	Sedimentation rate method	TOC (% dry mass)	TOC accumulation rate (mg C cm^{-2} year^{-1})	Grain size	Sediment depth (cm)	Study
Naples Bay, FL	Gordon River	River-dominated	Layered and fine-grained	0.3	^{210}Pb, penetration depth assumed 100 y			42% fines	0-54	Van Eaton et al. 2010
	Haldeman Creek	Tidal creek	Sandy with oyster shell and lenses of organic matter	0.2				20% fines	0-34	
	Naples Bay	Embayment	Decrease in fines downward	0.3					0-23	
	Dollar Bay	Embayment	Sandy with oyster shell and lenses of organic matter	0.3				20% fines	0-38	
Charlotte Harbor, FL		Microtidal, river dominated	Sandy	0.27	^{210}Pb	1.04 - 1.09	3.72	97% sand, 0.49-3.9 % clay	0-50	Turner et al. 2006
Tampa Bay, FL	Hillsborough Bay, Old Tampa Bay	Sediment-starved	Terrigenous clastic mud facies	0.13 - 0.42	^{210}Pb	1.5 - 2.5		4-7 phi	0-100	Brooks and Doyle 1998
Tampa Bay, FL		Microtidal	Coarse	1.1	^{239,240}Pu normalized to Al			coarse	0-51	Santschi et al. 2001
Apalachicola Bay, FL	River Mouth	River-dominated	Clay-dominated	1.53	^{210}Pb	0.4 - 5.8	3.1 - 10	30-60% clay	0-55	Surratt et al. 2008
	Dry Bar	River-dominated	Clay-dominated	1.24	^{210}Pb	2.1-2.5	0.5 - 42	80% clay	0-55	
	East Bay	River-dominated	Clay-dominated	1.26	^{210}Pb	1.75 - 2	0.7 - 29	50-70% clay	0-55	
Mississippi Sound, AL	Bayou la Batre	Lagoon	Sand-dominated, more fines with depth	0.11 - 0.48	^{210}Pb normalized to silt + clay	0.13 - 0.61	0.7 - 4.7	12-30% fines	0-122	This study
Grand Bay, MS	Bayou Heron	Tidal creek	Sand-dominated 0-40 cm, silt-dominated below	0.2		0.47 - 2.45	0.4 - 5.6	30-40% fines except silt layer 28-60 cm deep	0-120	This study
	Bayou Cumbest	Tidal creek	Equal amounts sand and silt, 10% clay	0.34		0.86 - 2.02	1.5 - 10.5	50-60% fines	0-84	This study
	Point aux Chenes Bay	Lagoon	Equal amounts sand and silt above 19 cm, silt-dominated below	0.49		0.13 - 0.64	1.8 - 3.7	42-82% fines, increasing with depth	0-80	This study
	Bangs Lake	Tidal creek/ embayment	Variable, equivalent amounts sand, silt, clay	0.86		0.61 - 1.00	3.4 - 10.9	32-63% fines, variable with depth	0-86	This study
Bayou Chico, MS	Bayou Chico	Tidal creek	45-90% sand; usually >70% sand and 30% fines	0.32		0.51 - 2.60	3.3 - 9.5	11-30% fines, 30% silt layer at 14-16 cm	0-57	This study

Table 2. Regression parameters for excess texture-normalized ^{210}Pb ($^{210}Pb_{normalized}$) versus sediment depth (Fig. 3). Exponential model used the form $y = ae^{-bx}$; y = excess $^{210}Pb_{normalized}$, x = sediment depth (cm); a (y-intercept) and b (slope) parameters are noted in table. AR is mean sediment accumulation rate calculated according to: $AR = {}^{-\lambda}/_{b}$ where λ is the decay constant of ^{210}Pb = 0.03114 y^{-1}, and b is the slope of the exponential decay model.

Site	a	b	r^2	p	AR (cm y^{-1})
Point aux Chenes Bay	0.015	0.064	0.73	0.01	0.49
Bayou la Batre 1	0.093	0.065	0.68	0.02	0.48
Bayou la Batre 2	0.179	0.290	0.71	< 0.01	0.11
Bayou Heron	0.047	0.156	0.72	< 0.01	0.20
Bayou Cumbest	0.034	0.102	0.88	< 0.01	0.34
Bangs Lake	0.027	0.036	0.84	< 0.01	0.86
Bayou Chico	0.162	0.098	0.87	< 0.01	0.32

06 **Table 3.** Comparison of mean (± SE) sediment core characteristics between (a) tidal
07 creek (HE, CU, CH) and open water sites (PC, BA, BB1, BB2) and (b) impacted (CH,
08 BB1, BB2) and reserve sites (PC, HE, CU, BA).

(a)

Parameter	Creek	Open
% TOC	1.38 ± 0.18	0.51 ± 0.16
%TN	0.081 ± 0.014	0.05 ± 0.01
C:N	20.39 ± 0.82	11.55 ± 0.71
$\delta^{13}C$	-25.45 ± 0.53	-22.74 ± 0.47
$\delta^{15}N$	3.46 ± 0.60	3.70 ± 0.52
Cp	7.13 ± 1.44	5.18 ± 1.24

(b)

	Impacted	Reserve
% TOC	0.88 ± 0.35	0.88 ± 0.30
% TN	0.067 ± 0.018	0.061 ± 0.015
C:N	13.3 ± 2.8	16.9 ± 2.5
$\delta^{13}C$	-23.52 ± 1.03	-24.20 ± 0.90
$\delta^{15}N$	4.46 ± 0.33	2.95 ± 0.28
Cp	8.15 ± 0.95	4.41± 0.82

09
10

Table 4. Environmental parameters for water column (June – September 2011, n = 8 dates) and stable isotope ratio differences between bottom water SPM and surface sediments (n = 3 dates). $\delta^{13}C_{SPM\text{-}Sed}$ was correlated with temperature (r = 0.60), SPM C content (r = 0.60), SPM N content (r = 0.60), and SPM C:N (r = 0.59). $\delta^{15}N_{SPM\text{-}Sed}$ was negatively correlated with static stability (stratification) (r = -0.62).

Site	Depth (m)	Salinity	Temp (ºC)	Static Stability	$\delta^{13}C_{SPM\text{-}Sed}$	$\delta^{15}N_{SPM\text{-}Sed}$
BA	0.65 ± 0.07	22.5 ± 1.1	30.3 ± 0.7	0.0002 ± 0.0004	-2.87	4.91
BAU	0.71 ± 0.03	22.9 ± 1.1	29.3 ± 0.5	0.0007 ± 0.0005	-2.86	2.24
CH	0.86 ± 0.12	22.1 ± 2.0	30.4 ± 0.5	0.0010 ± 0.0004	-2.74	1.80
CHU	0.24 ± 0.03	21.0 ± 1.8	32.0 ± 0.9	0.0020 ± 0.0020	-1.70	2.09
CU	0.69 ± 0.05	22.9 ± 1.3	29.5 ± 0.5	0.0006 ± 0.0005	-4.64	1.77
CUU	0.81 ± 0.05	21.0 ± 1.2	30.2 ± 0.5	0.0022 ± 0.0014	-2.11	2.43
HE	0.50 ± 0.05	21.8 ± 1.4	29.2 ± 0.4	0.0009 ± 0.0006	-3.49	1.51
HEU	1.61 ± 0.07	21.3 ± 1.0	30.0 ± 0.6	0.0047 ± 0.0016	-4.11	0.22
PC	1.38 ± 0.05	23.5 ± 1.7	29.7 ± 0.7	0.0002 ± 0.0001	-2.34	2.03
Mean	**1.15 ± 0.15**	**22.1 ± 0.3**	**30.1 ± 0.3**	**0.00138 ± 0.0005**	**-2.99 ± 0.32**	**2.11 ± 0.11**

Table 5. Correspondence between time periods of greatest measured change in sediment attributes and documented land use at tidal creek and open water sites near Grand Bay, Mississippi on the northern Gulf of Mexico coast. R = Reserve sites; I = Impacted sites; nd = core section not dated earlier than confidence limits.

Site (impact category)	Time period at maximum value or change in value (confidence limits)						Corresponding land-use change
	%TOC	%TN	C:N	$\delta^{13}C$	$\delta^{15}N$	*C. perfringens*	
Tidal creek							
HE (R)	nd – 1916	1916	nd – 1916	nd – 1916	1916	peaks 1941, earlier	Hydrology assoc. w/ railroad[1]/I-90[2] development
	(nd – 1946)	(nd – 1946)	(nd – 1946)	(nd – 1946)	(nd – 1946)	(nd – 1964)	
CU (R)	1897 – 1956	1996	1897 – 1956	1897 – 1956	nd	1996	Hydrology assoc. w/ railroad/I-90 development; failing septic (1990s)[3]
	(nd – 1970)	(1987 – 2004)	(nd – 1970)	(nd – 1970)		(1987 – 2004)	
BA (R)	1966 – 1989	1966 – 2010	1966	1966 – 1989	1989	2010	Industrialization (MS Phosphates, Chevron, Shipyard)[4]
	(1925 – 2000)	(1925 – 2000)	(1925 – 1983)	(1925 – 2000)	(1973 – 2000)		
CH (I)	1954 – 1985	1985 – 1997	1954	variable throughout	2011	1954	Industrialization (see BA) and urbanization (Pascagoula)
	(1920 – 1993)	(1972 – 2007)	(1920 – 1969)			(1920 – 1969)	
Open water							
BB1 (I)	2010	nd – 1972	nd	1951 – 1972	2010	2010	Industrialization and urbanization (Bayou la Batre)[5]
		(nd – 1992)	(nd – 1951)	(nd – 1992)		peak 1992	
BB2 (I)	2010	2010	nd	nd	2010	2010	
			(nd – 1920)				
PC (R)	2010	2010	nd – 1924		nd – 1924	2010	Little change through time

[1] Hancock County Historical Society
[2] Sullivan 2007, Woodrey 2007b
[3] LaSalle 1997
[4] USGS 1940, 1952, 1977
[5] NPDES AL0078921

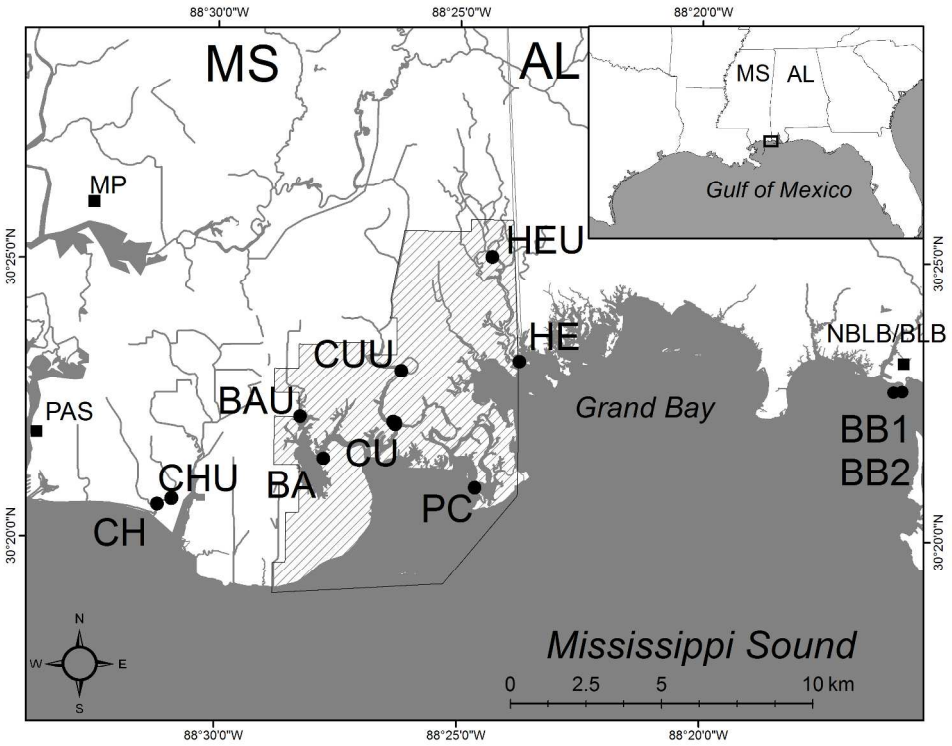

Fig. 1. Site map of sediment coring locations (triangles) in the Grand Bay National Estuarine Research Reserve, MS (GBNERR, hatched), and surrounding areas. From west to east: Bayou Chico (CH), Bangs Lake (BA), Bayou Cumbest (CU), Point aux Chenes Bay (PC), Bayou Heron (HE), Bayou la Batre (BB1 and BB2). Circles and site names are sites where suspended particulate matter (SPM) samples were collected, with "U" designating an upstream site in each tributary. Squares are locations of present-day wastewater treatment plants Pascagoula (PAS), Moss Point (MP), and Bayou la Batre (BLB).
Fig. 1
279x215mm (300 x 300 DPI)

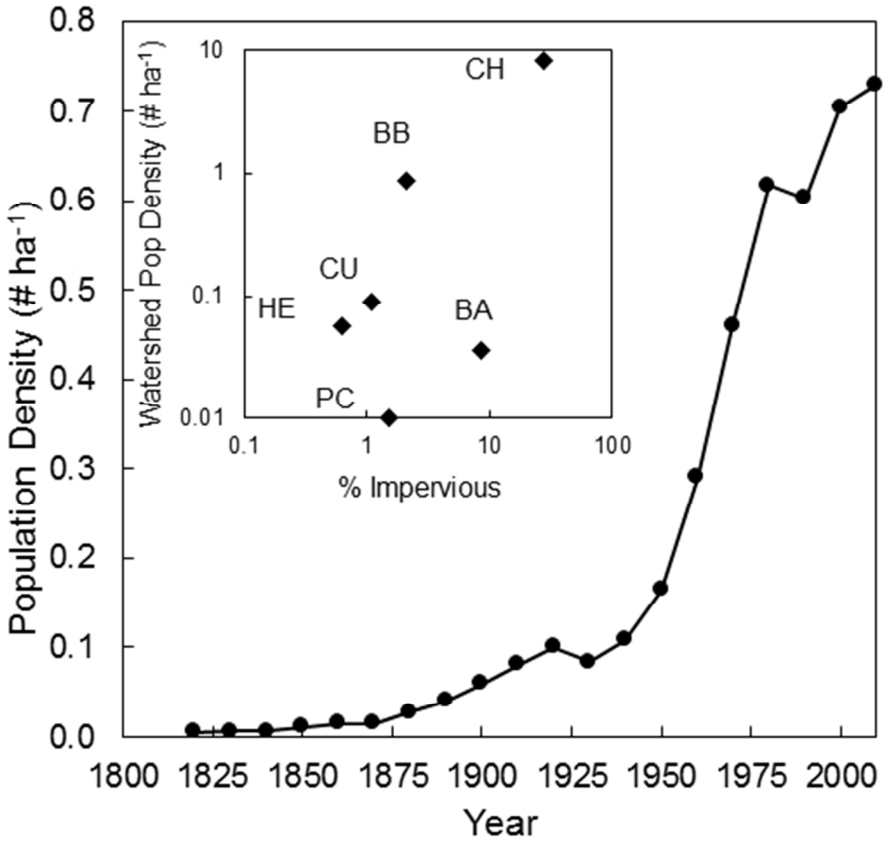

Figure 2. Population density of Jackson County, MS through the time (2010 census data: Minnesota Population Center 2011). Major population increases were in early 1900s, 1950s, and 1990s. Inset: Coring sites characterized by 2011 population density vs. impervious surface for each watershed (impervious surface land cover data: Homer et al. 2015). These data, plus GBNERR boundaries, led to site designations of "reserve" (PC, HE, CU, BA) or "impacted" (CH, BB). (C) Jackson County fertilizer use, 1987-2006 (Gronberg and Spahr 2012).

Fig. 2

152x152mm (96 x 96 DPI)

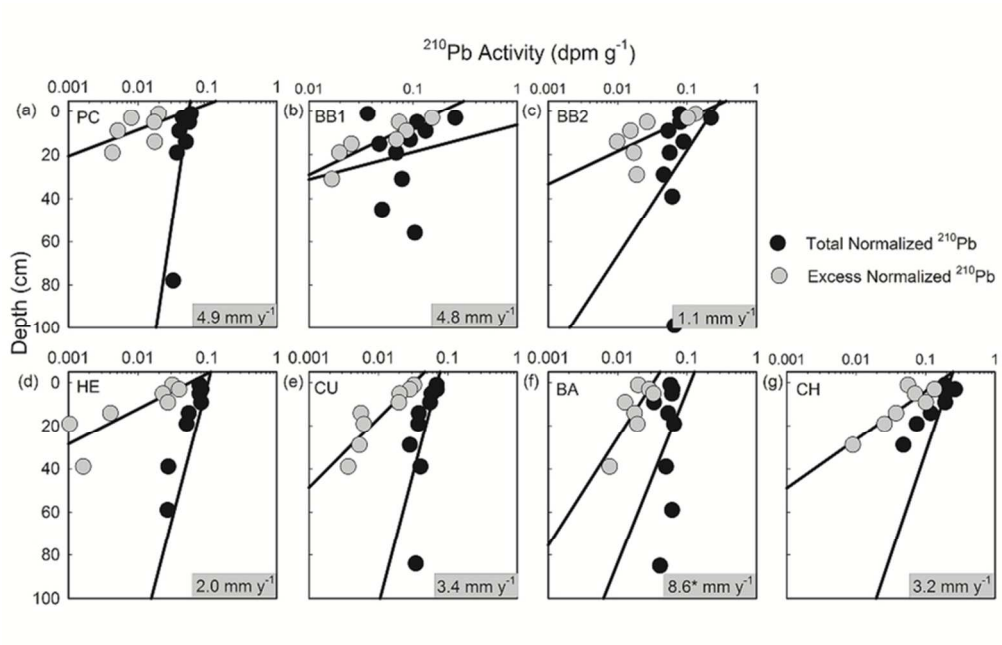

Figure 3. Total and excess ^{210}Pb activity (disintegrations per minute per gram dry sediment, dpm g^{-1}), normalized for sediment texture (silt + clay content, see methods) vs. depth down-core at each site. Excess $^{210}Pb_{normalized}$ (Total – Supported $^{210}Pb_{normalized}$) was used to calculate sediment accumulation rates and dates using an exponential regression (Table 1). Mean sediment accumulation rate is inset on lower right for each site. *Calculated accumulation rate for BA may be inaccurate due to contamination by phosphogypsum – processing facility, artificially elevating ^{210}Pb (see Discussion for details).

Fig. 3
40x26mm (600 x 600 DPI)

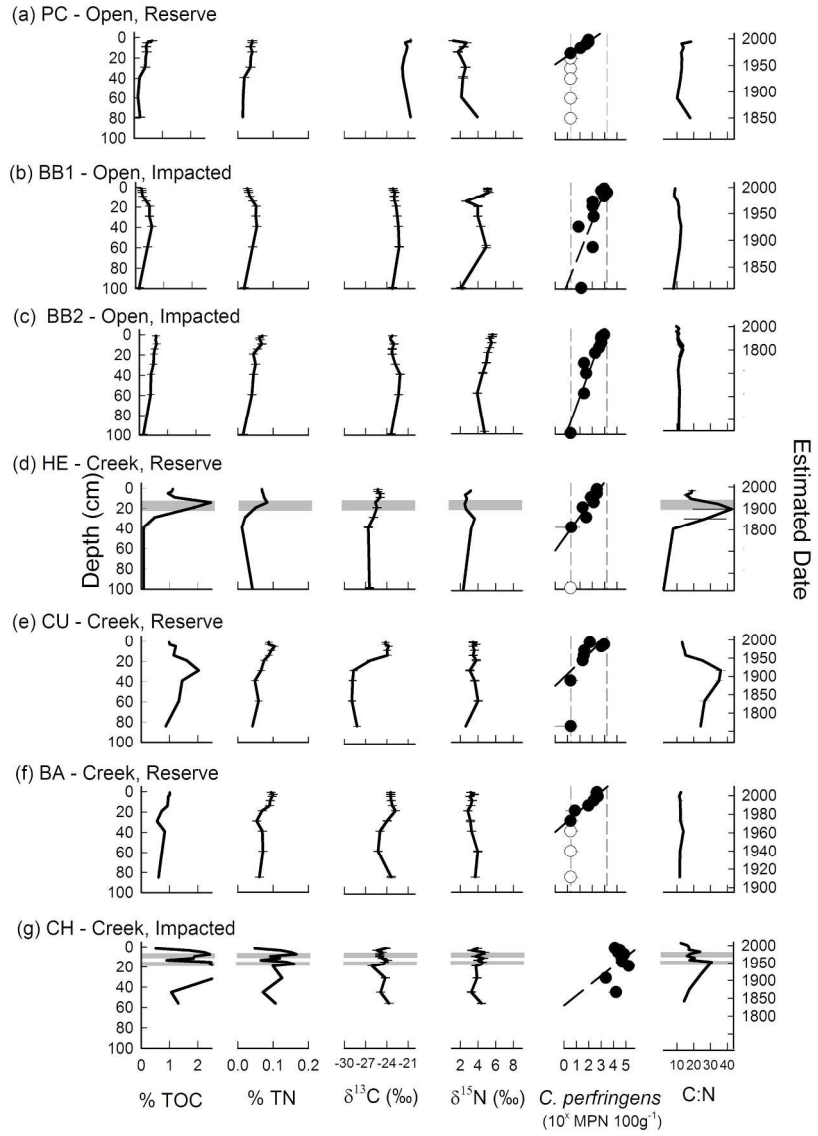

Figure 4. Down-core profiles of sediment %TOC, %TN, $\delta^{13}C$, $\delta^{15}N$, C. perfringens and molar C:N with sediment depth. Estimated date ($CIC_{normalized}$ method) on right-hand y-axis. Open-water sites (top to bottom: PC, BB1, BB2), followed by tidal creek sites (HE, CU, BA, CH). Gray shaded bars where changes in sediment grain size, %TOC and C:N were noted, possibly hurricane event layers. For *C. perfringens*, lower and upper detection limits indicated by vertical dashed lines; samples below detection limits: white symbols. Significant regressions have lines of best fit as solid lines; dashed lines of best fit are used to demonstrate non-steady state periods.

Fig. 4
215x275mm (300 x 300 DPI)

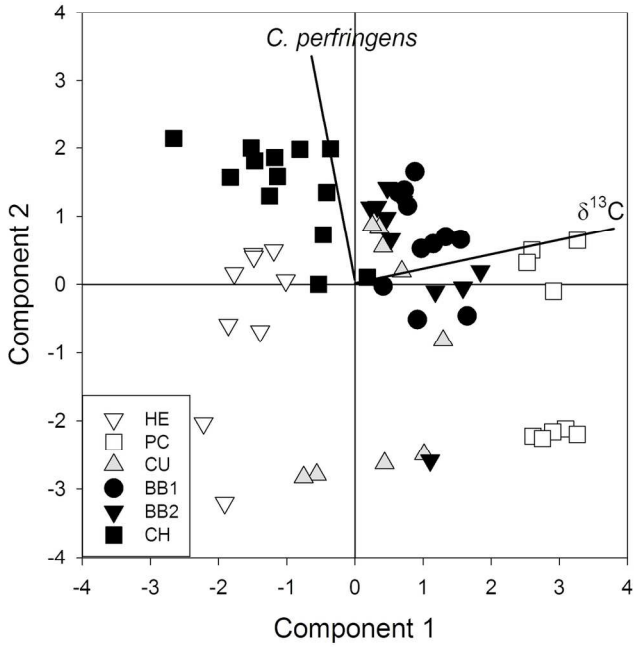

Figure 5. Principal components analysis: C. perfringens, %TOC, %TN, $\delta^{13}C$, $\delta^{15}N$, % sand, % water. Symbols represent sediment core samples from different sites. Component 1 explained 58.6% of the variance (eigenvalue = 3.29); Component 2 explained 38.1% of the variance (eigenvalue = 2.14). Component 1 was primarily explained by $\delta^{13}C$ (loading = 0.98), and Component 2 was primarily explained by *C. perfringens* (loading = 0.97). $\delta^{13}C$ separated open water (PC, BB1, BB2) from tidal creek sites (CH, CU, HE), with BA intermediate. *C. perfringens* separated reserve (PC, HE, BA) from impacted sites (CH, BB1, BB2) with site CU intermediate.
Fig. 5
152x197mm (300 x 300 DPI)

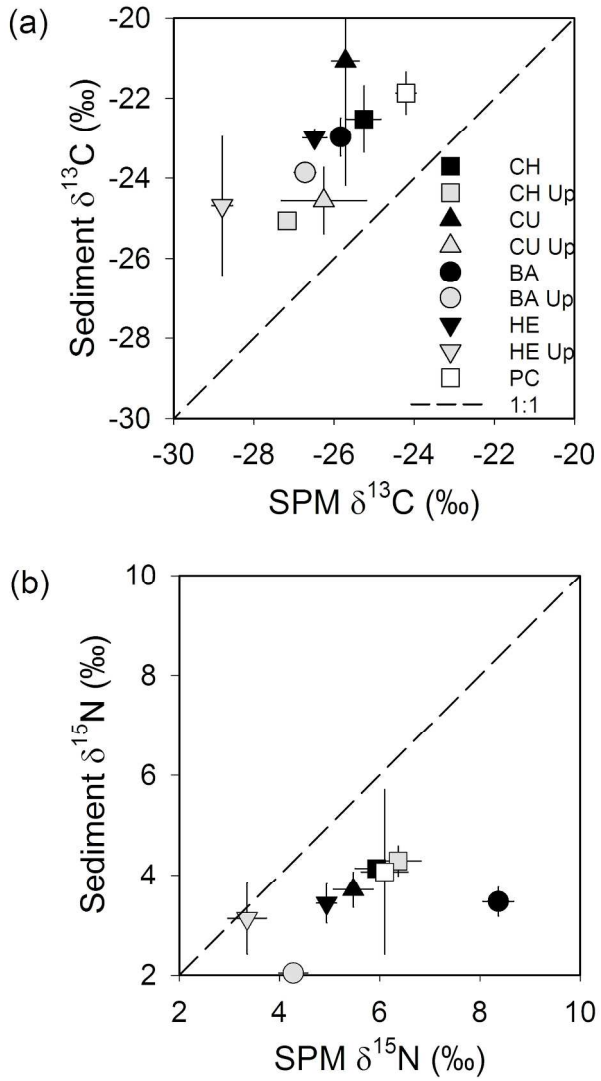

Figure 6. Mean values for (a) $\delta^{13}C$ and (b) $\delta^{15}N$ of organic matter from surface sediments (y-axes) plotted against values from suspended particulate matter (SPM; x-axes) for locations downstream or upstream (indicated by UP in the legend) from each of the coring sites. Each point is an average of 3 replicate samples for sediment and SPM. Samples were collected in May-September 2011. SPM had consistently lower $\delta^{13}C$ and higher $\delta^{15}N$ than sediments, as indicated by 1:1 lines (dashed). Upstream sites had lower $\delta^{13}C$ than downstream sites, but upstream-downstream patterns were not evident for $\delta^{15}N$.
Fig. 6
152x289mm (300 x 300 DPI)

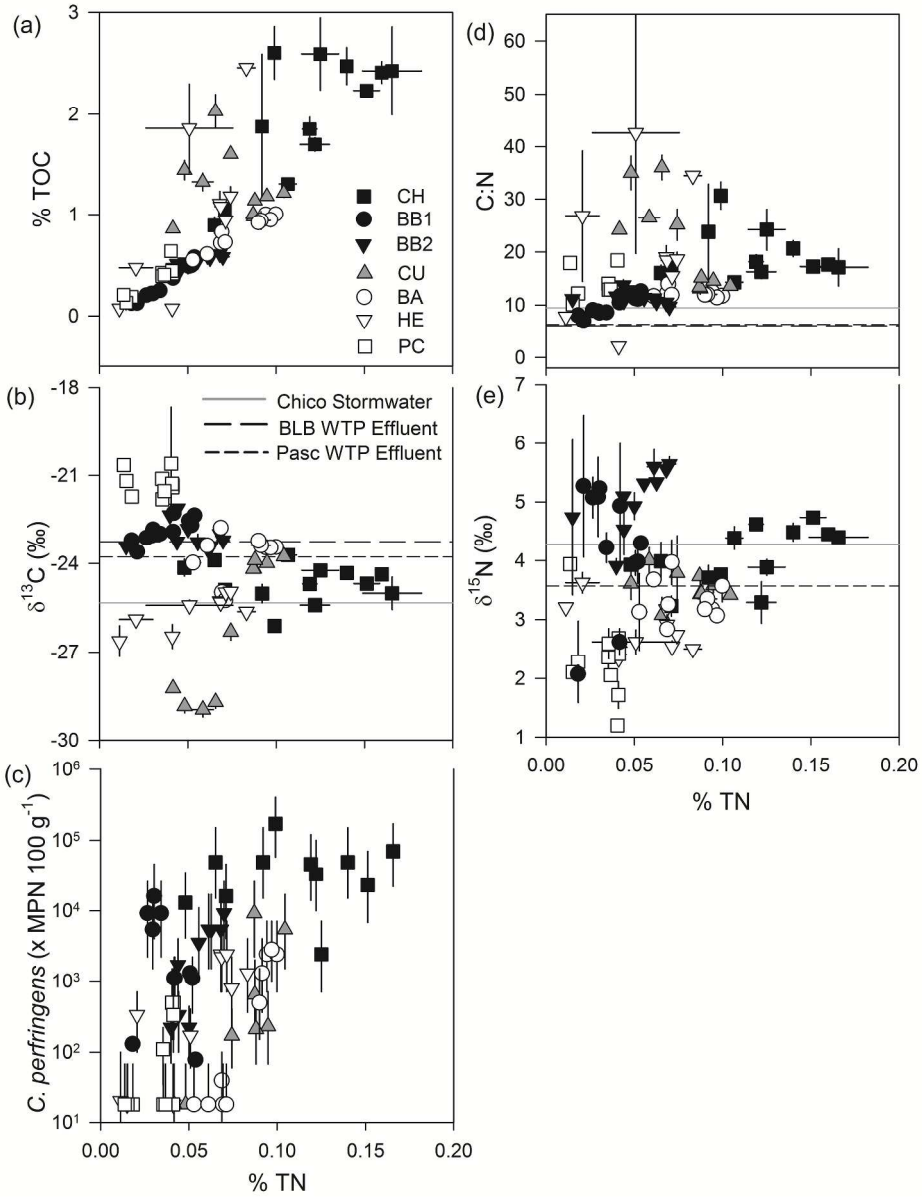

Figure 7. Comparisons between sediment core characteristics and %TN. Sites are grouped by hypothesized anthropogenic impact: more (dark symbols) to less (white symbols). C:N and stable isotope values are indicated for three potential anthropogenic organic matter sources (Bayou Chico stormwater, Bayou la Batre WTP effluent, Pascagoula WTP effluent).

Fig. 7

129x165mm (600 x 600 DPI)

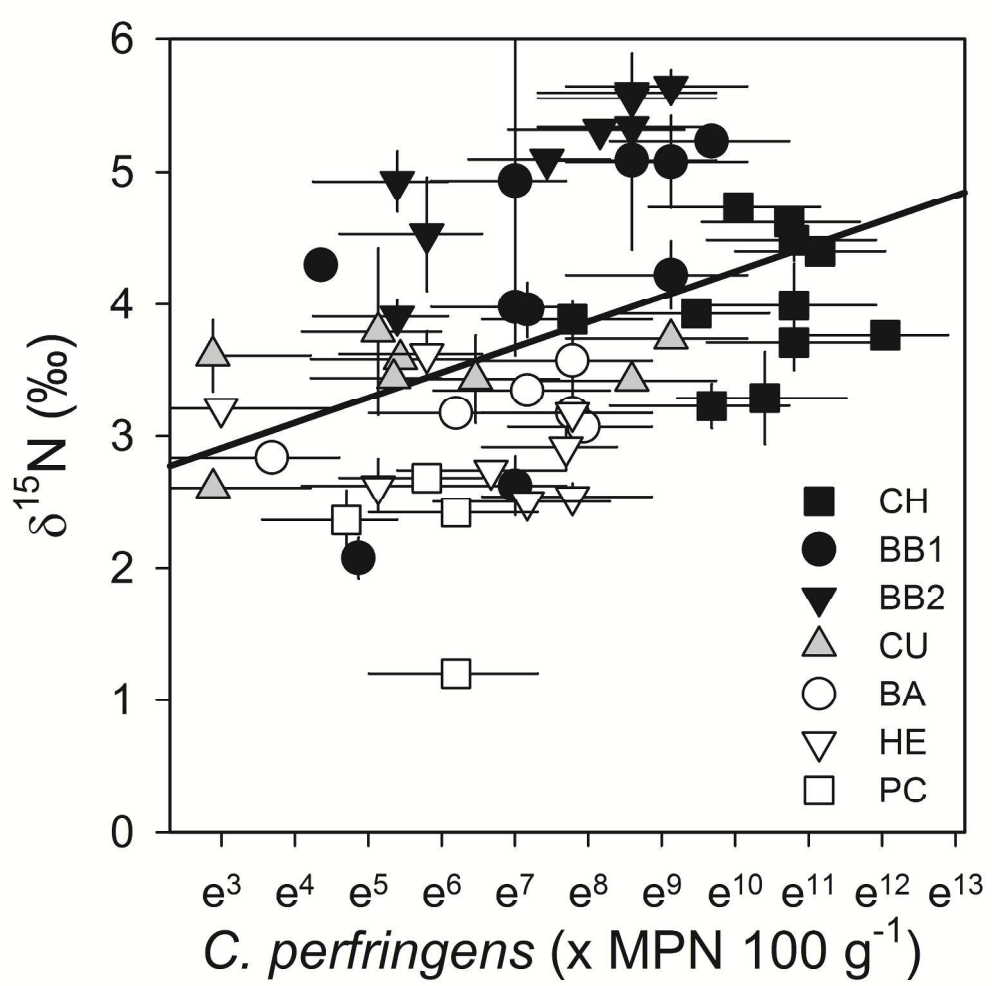

Figure 8. Correlation between potential wastewater indicators $\delta^{15}N$ and ln(*C. perfringens*) densities for all sites and sediment core layers. Symbols for hypothesized wastewater-influenced sites are black; hypothesized non-wastewater-influenced sites have white symbols; We hypothesize that Bayou Cumbest is impacted by intermediate wastewater influence (gray symbols).

Fig. 8

Table S1. Sediment physical parameters, radioisotopes, and estimated date ranges. BD = below detection, nd = not dated.

Site Name	Depth (cm)	Bulk Density (g cm^{-3})	% Water	% Sand	% Silt	% Clay	Sediment Color	Comments	^{137}Cs	Cl ^{137}Cs	Earliest Date (^{137}Cs)	^{210}Pb Normalized	Predicted Excess ^{210}Pb Normalized	Date Excess ^{210}Pb normalized	Date Range
Point Aux Chenes Bay	0-2	0.86	27.5	57.8	30.3	11.9	10YR 4/1	Grass debris; Brownish gray	BD	BD	nd	0.020	0.014	2009	1942 - 2011
(PC)	2-4	1.18	27.4	54.3	36.6	9.2	10YR 4/1		BD	BD	nd	0.008	0.012	2005	1963 - 2011
6/16/2011	4-6	1.04	28.7	56.8	37.9	5.4	10YR 4/1	Brownish gray	BD	BD	nd	0.017	0.011	2001	1968 - 2011
	8-10	1.35	27.1	46.6	46.8	6.6	10YR 4/1		BD	BD	nd	0.005	0.008	1993	1951-2010
	13-15	0.96	28.4	40.4	53.6	6	10YR 4/1		BD	BD	nd	0.017	0.006	1982	BD - 2007
	18-20	2.60	25.6	45.6	49.1	5.3	10YR 6/1	Light brownish gray	BD	BD	nd	0.004	0.004	1972	BD - 2004
	28-30	1.64	23.9	40.0	55.2	4.9	10YR 4/1	Brownish gray	nd	nd	nd	nd	nd	nd	nd
	38-40	1.85	19.0	16.0	77.2	6.8	10YR 4/1		nd	nd	nd	nd	nd	nd	nd
	48-50	1.82	18.3	17.9	71.9	10.1	10YR 5/1	Light brownish gray	nd	nd	nd	nd	nd	nd	nd
	58-60	2.06	16.6	18.1	63.7	18.2	10YR 5/2	Grayish yellow brown	nd	nd	nd	nd	nd	nd	nd
	76-80	2.09	15.4	18.2	62.8	19	10YR 5/3	Dull yellowish brown	BD	BD	nd	-0.001	0.000	1851	nd - 1924
Bayou la Batre	0-2	1.11	25.3	88.1	7	4.9	N3	Small shell debris, soupy, dark gray	BD	BD	2011	0.056	0.088	2009	1977 - 2011
(BB1)	2-4	0.66	27.4	86.2	6.5	7.2	N3		BD	BD	2002	0.134	0.077	2005	1978 - 2011
6/23/2011	4-6	0.77	28.2	85.2	9.3	5.6	N3	Soupy, dark gray	BD	BD	1993	0.070	0.068	2001	1977 - 2011
	8-10	0.71	27.3	80.1	12.1	7.8	N3	Dark gray	BD	BD	1976	0.101	0.052	1992	1969-2006
	13-15	0.90	29.4	75.4	16.9	7.7	5GY 4/1	Dark gray-green	0.12	0.02	1954	0.038	0.038	1982	1947-1998
	18-20	0.81	36.3	57.4	31.3	11.3	N4		BD	BD	nd	0.026	0.027	1972	1896-1992
	28-30	1.43	32.3	64.3	29.9	5.8	N5	Gray	BD	BD	nd	0.009	0.014	1951	nd-1980
	38-40	1.16	33.9	54.8	38.7	6.5	N4		nd	nd	nd	nd	nd	nd	nd
	58-60	1.46	29.7	69.8	23.2	7	N5		nd	nd	nd	nd	nd	nd	nd
	98-100	1.62	23.5	63.6	19.6	16.8	5Y 5/4; 2.5Y 7/8; 10R 4/6	Whole shell at 75 cm; Color change to orange/red at 74 cm	nd	nd	nd	nd	nd	nd	nd
	120-122	1.17	nd	37.2	35.5	27.3	N7; 7.5 YR 6/8; 7.5 YR 5/2	Marbled colors	BD	BD	nd	0.024	nd	nd	nd
Bayou la Batre	0-2	0.60	41.1	71.1	15.9	13	5G 4/1	Dark greenish-gray	BD	BD	2011	0.133	0.134	2002	1972 - 2011
(BB2)	2-4	0.68	38.5	88.1	0	11.9	5G 4/1	mall shell pieces; dark greenish-gra	0.21	0.03	2002	0.103	0.075	1983	1963-1996
6/23/2011	4-6	0.51	38.0		nd		5GY 4/1	Dark greenish-gray	BD	BD	1993	0.027	0.042	1965	1933-1982
	8-10	0.79	14.1	64.1	24.8	11.1	5GY 4/1		0.14	0.02	1976	0.015	0.013	1927	nd-1955
	13-15	0.65	50.9	54.4	28.8	16.8	5GY 4/1	mall shell pieces; dark greenish-gra	0.48	0.04	1954	0.010	0.003	1881	nd-1920
	18-20	1.12	34.7	74.7	19.9	5.4	5GY 4/1	Dark greenish-gray	BD	BD	nd	0.017	0.001	nd	nd
	28-30	0.89	38.5	62.1	25.8	12.1	5GY 4/1		BD	BD	nd	0.019	0.000	nd	nd
	38-40	1.29	35.0	68.5	16.6	14.9	5YR 5/1; 5G 4/1	Copper-colored red in dark sedimen	BD	BD	nd	0.016	0.000	nd	nd
	58-60	1.25	33.4	65.4	28.8	5.8	5G 4/1	Dark greenish-gray	nd	nd	nd	nd		nd	nd
	98-100	1.59	23.9	73.4	18.1	8.5	10YR 7/8; 10YR; 10R 3/6; N7	Pieces of red material - wood?	BD	BD	nd	0.002		nd	nd
Bayou Heron	0-2	0.56	28.7	57.2	25.6	17.2	10YR 2/1		BD	BD	2011	0.031	0.040	2006	1979 - 2011
(HE)	2-4	0.74	28.3	58.3	31.3	10.5	10YR 2/1	Lot of shell, Black	0.18	0.03	1983	0.039	0.029	1996	1975-2009
6/16/2011	4-6	1.07	27.9	68.8	21.3	9.9	10YR 2/1		0.28	0.03	1954	0.023	0.021	1986	1967-2000
	8-10	1.13	30.0	66.4	26.5	7.2	10YR 4/1	Lot of shell - oyster, clam, wood, Brownish-gray	BD	BD	nd	0.027	0.011	1966	1931-1982
	13-15	1.15	36.3	61.1	28.6	10.3	10YR 4/1	, debris, oyster shell, seed, Brownis	BD	BD	nd	0.004	0.005	1941	nd-1964
	18-20	0.95	38.5	60.8	25.1	14	10YR 2/1	aves, lot of debris, wood, shell, Bla	BD	BD	nd	0.001	0.002	1916	nd-1946
	28-30	1.77	26.3	15.7	59.9	24.3	10YR 4/1	Wood pieces, Brownish-gray	nd	nd	nd	nd	nd	nd	nd
	38-40	2.77	18.6	7.9	71.1	21	10YR 6/1		BD	BD	nd	0.002	0.000	nd	nd
	58-60	2.42	19.2	16.2	59.9	23.9	10YR 6/1	Brownish-gray	BD	BD	nd	0.007	0.000	nd	nd
	98-100	1.85	18.4	90.5	6.2	3.3	10YR 6/1		nd	nd	nd	nd	nd	nd	nd
	118-120	2.16	20.4	61.1	29.7	9.3	10YR 6/1	Stick, Brownish-gray	nd	nd	nd	nd	nd	nd	nd
	138-140	2.47	18.6	64.0	29.3	6.7	7.5YR 6/1	Brownish-gray	nd	nd	nd	nd	nd	nd	nd
	158-160	1.43	19.1	49.9	43.5	6.6	10YR 6/1	Roots, Brownish-gray	BD	BD	nd	0.005	0.000	nd	nd
Bayou Cumbest	0-2	0.43	39.7	39.5	19.3	41.2	10YR 2/1	Oyster drill shell; Black	BD	BD	2011	0.033	0.031	2008	1995 - 2011

(CU)	2-4	0.71	36.9	53.4	38	8.6	5Y 2.5/2	Olive black	0.20	0.03	1997	0.028	0.026	2002	1991 - 2011
6/9/2011	4-6	0.59	37.7	40.0	44.4	15.6	5Y 2.5/2	Olive black; Oyster shells at 6-8 cm	0.15	0.02	1983	0.020	0.022	1996	1987 - 2004
	8-10	0.73	38.9	43.0	45.8	11.1	5Y 2.5/2	Olive black	0.21	0.03	1954	0.020	0.015	1985	1974 - 1992
	13-15	0.84	35.4	38.3	48.3	13.4	5Y 2.5/2	Big piece of oyster shell; olive black	BD	BD	nd	0.006	0.010	1970	1953 - 1982
	18-20	1.91	30.4	45.7	45.7	8.6	5Y 2.5/2	Shell pieces; olive black	BD	BD	nd	0.006	0.006	1956	1926 - 1970
	28-30	1.60	8.2	39.5	46.4	14.1	5Y 2.5/2	Olive black	BD	BD	nd	0.005	0.002	nd	nd
	38-40	2.05	22.2	48.1	42.3	9.6	5Y 2.5/2	Marbled light & dark brown	BD	BD	nd	0.004	0.001	1897	nd-1948
	58-60	1.92	28.1	38.0	43.6	18.5	10YR 4/1	Grass, brownish-gray	nd	nd	nd	nd	nd	nd	nd
	83-85	1.62	25.0	39.6	60.3	0.1	10YR 4/1		BD	BD	nd	0.001	0.000	nd	nd - 1948
Bangs Lake	0-2	0.42	36.9	47.4	27.1	25.5	5GY 4/1	Shell at surface, dark olive gray	0.45	0.06	2011	0.020	0.026	2010	1993 - 2011
(BA)	2-4	0.82	35.8	53.4	30.4	16.2	5GY 4/1	Small shell pieces, dark olive gray	0.22	0.03	2005	0.028	0.024	2007	1992 - 2011
6/9/2011	4-6	0.74	35.9	46.5	40.4	13.1	7.5YR 2.5/1	Black	0.24	0.03	1998	0.033	0.022	2005	1990 - 2011
	8-10	0.96	34.1	27.6	31.5	40.9	10YR 2/1		0.30	0.03	1986	0.013	0.019	2001	1986-2010
	13-15	0.00	0.0	58.8	35.2	6	10YR 4/1		0.23	0.03	1970	0.018	0.016	1995	1980-2004
	18-20	1.76	16.1	68.5	20.1	11.5	10YR 4/1	Brownish gray	0.16	0.02	1954	0.019	0.013	1989	1973-2000
	28-30	1.28	17.9	63.9	29.4	6.6	10YR 4/1		nd	nd	nd	nd	nd	nd	nd
	38-40	1.14	32.8	41.9	49.9	8.3	2.5Y 4/2	Plant pieces (roots, stems), dark grayish yellow	BD	BD	nd	0.008	0.006	1966	1925-1983
	58-60	1.34	30.4	43.5	50.1	6.4	5GY 4/1	nt pieces (roots, stems), dark olive g	BD	BD	nd	0.013	0.003	1942	nd-1966
	84-86	1.55	30.3	36.8	36.3	26.9	2.5Y 8/8 in 5GY 4/1	Yellow/gray marbled color	BD	BD	nd	0.000	0.001	1912	nd-1944
Bayou Chico	0-2	1.35	27.0	88.8	3.4	7.8	5Y 2.5/2	Top 2 cm oxidized layer, black	BD	BD	nd	0.023	0.147	2010	nd
(CH)	2-4	0.86	39.4	72.6	14.5	12.9	N 2.5/	Leaves, roots, black	BD	BD	nd	0.152	0.121	2004	1986 - 2013
6/19/2013	4-6	1.16	44.3	70.1	14.2	15.7	N 2.5/	Large stems, black	BD	BD	nd	0.073	0.099	1997	1983-2007
	6-8	1.12	43.4	72.0	13	15	N 2.5/	Small roots, black	nd	nd	nd	nd	nd	nd	nd
	8-10	1.05	34.2	70.5	15.5	14	N 2.5/	Leaves & stems, black	BD	BD	nd	0.086	0.067	1985	1972-1993
	10-12	0.97	38.7	69.9	21.6	8.6	N3/	Piece of wood, black	nd	nd	nd	nd			
	12-14	1.11	31.3	76.1	12.9	10.9	N3/	Leaves, black	BD	BD	nd	0.069	0.046	1972	1956-1983
	14-16	0.83	43.9	61.1	27.4	11.5	5GY 5/1, N4/	Dark green-gray, medium gray	BD	BD	nd	0.025	0.038	1966	1946-1978
	16-18	0.78	48.3	79.2	12.3	8.5	N3/	Small roots, black	nd	nd	nd	nd	nd	nd	nd
	18-20	0.97	38.5	75.5	14.3	10.2	N2.5/	Large section of leaves at 20 cm, black	BD	BD	nd	0.020	0.025	1954	1920-1969
	30-32	0.96	39.9	75.5	15.8	8.7	5GY 4/1		BD	BD	nd	0.017	0.008	1916	nd-1942
	44-46	1.04	7.8				5GY 4/1	Dark olive gray	BD	BD	nd	0.004	0.002	1872	nd-1907
	55-57	0.77	37.4	76.9	11.7	11.4	5GY 4/1		BD	BD	nd	0.043	nd	nd	nd

Table S2. Stable isotope values and C:N for potential anthropogenic particulate organic matter source material to the study area. We did not find significant sources of stormwater to sites other than CH in our shoreline surveys.

Potential Source	$\delta^{13}C$ (‰)	$\delta^{15}N$ (‰)	C:N	Dates sampled	Sample Interval
Bayou la Batre WTP	-23.26 ± 0.40	8.27 ± 0.50	6.08 ± 0.24	6/4/12 - 10/2/12	Monthly
Moss Point WTP	-23.07 ± 0.15	5.92 ± 0.67	6.13 ± 0.15	5/7/12 - 5/1/13	Monthly
Pascagoula WTP	-23.77 ± 0.17	3.57 ± 0.48	6.33 ± 0.17	5/7/12 - 5/1/13	Monthly
Chico Stormwater	-25.33 ± 0.62	4.28 ± 0.32	9.46 ± 0.95	5/1/12 - 6/11/12	Biweekly

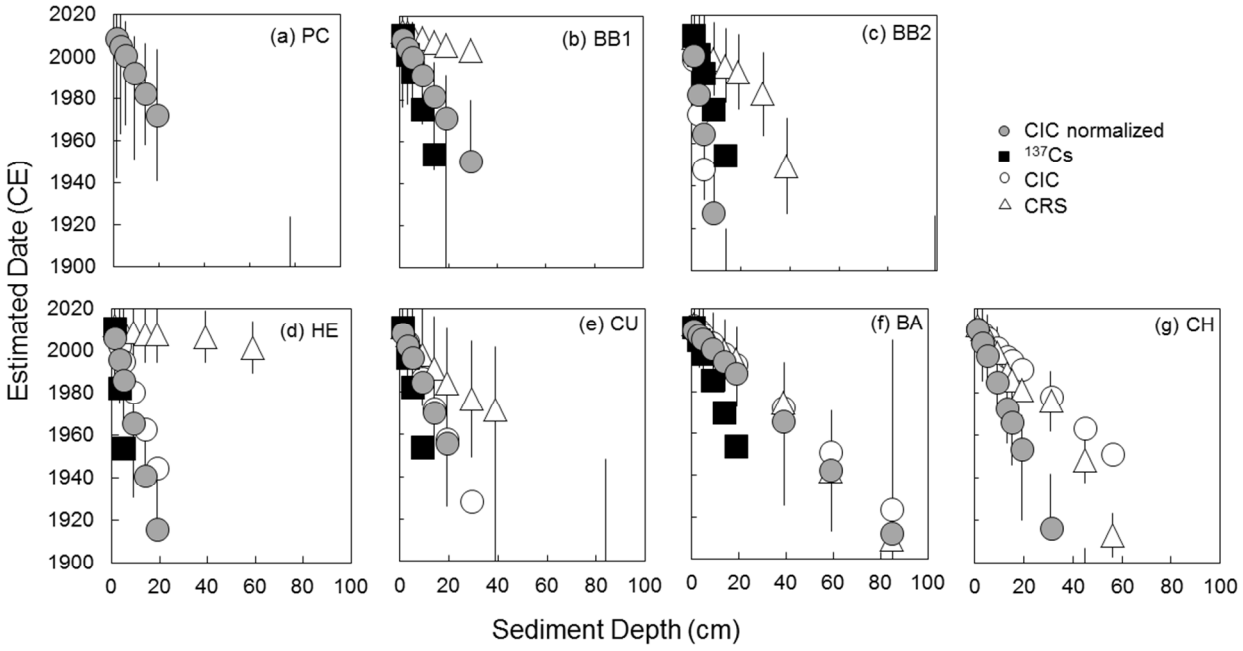

Figure S1. Estimated date ± 95% CI for each of four dating methods, including Constant Initial Concentration based on ^{210}Pb normalized to texture (CIC normalized), ^{137}Cs based on earliest observed ^{137}Cs and constant sedimentation rate, CIC based on non-normalized ^{210}Pb, and Constant Rate of Supply (CRS) based on non-normalized ^{210}Pb. ^{137}Cs could not be used at sites with non-detectable ^{137}Cs (PC and CH); CIC and CRS were not used when non-normalized $^{210}Pb_{excess}$ did not decrease logarithmically with depth (PC).

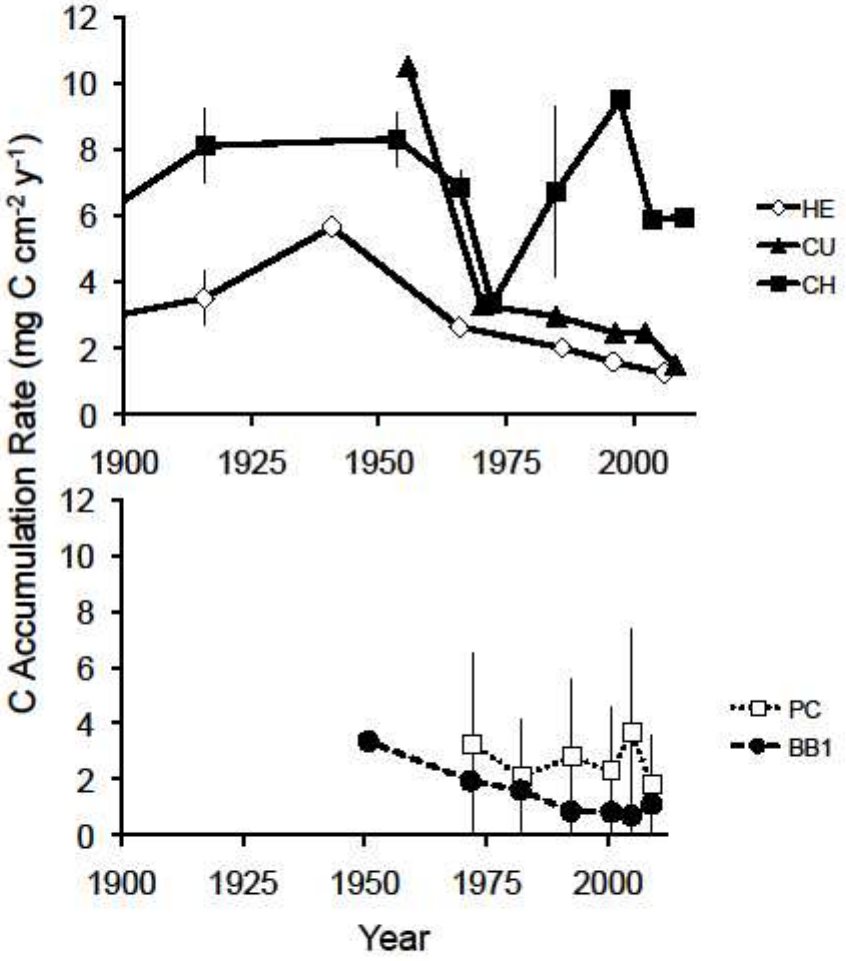

Figure S2. TOC accumulation rates in tidal creeks (upper panel) and open-water sediments (lower panel), calculated by sediment accumulation rate * bulk density * TOC concentration. Bayou Heron (HE), Bayou Cumbest (CU), and Point aux Chenes Bay (PC) are within GBNERR boundaries, while Bayou Chico (CH) and Bayou la Batre (BB1) are urbanized and wastewater-influenced sites outside reserve boundaries. TOC accumulation rates were higher in tidal creek than open water sediments, and have decreased in reserve tidal creek sediments since the 1960s. TOC accumulation remains high at the urbanized, high impervious surface tidal creek site Bayou Chico.